

A Theoretical Investigation of the  
Efficiency of a Moist Atmosphere

by

Dawna Lisa Paton

B.S., Massachusetts Institute of Technology  
(1977)

Submitted in Partial Fulfillment  
of the Requirements for the  
Degree of

Master of Science

at the

Massachusetts Institute of Technology  
(August, 1979)

Signature of Author \_\_\_\_\_  
Department of Meteorology, August, 1979

Certified by \_\_\_\_\_  
Thesis Supervisor

Accepted by \_\_\_\_\_  
Chairman, Department Committee

**WITHDRAWN**  
Indgren  
MASSACHUSETTS INSTITUTE  
OF TECHNOLOGY

**MIT LIBRARIES**  
1979  
LIBRARIES

A Theoretical Investigation of the Efficiency  
of a Moist Atmosphere

by

Dawna L. Paton

Submitted to the Department of Meteorology  
on August 27, 1979 in partial fulfillment of the  
requirements for the Degree of Master of Science

Abstract

The efficiency of a moist atmosphere is examined in an attempt to determine how close to maximum efficiency the atmosphere is operating. Since the efficiency may be expressed by the ratio of the rate of which the atmosphere generates kinetic energy to the rate of solar energy coming in at the top of the atmosphere, the rate of generation of moist available energy (MAE) must be estimated. The generation of MAE is associated with non-frictional heating and the release of latent heat energy. By assuming that all heating is due solely to long-wave radiation and specifying a relative humidity less than 90%, the problem is greatly simplified. Latent heat release need not be parameterized and clouds may be ignored. By ignoring ozone, using the observed mixing ratio of  $\text{CO}_2$ , the efficiency is solely a function of temperature and relative humidity. As such, the problem is reduced to finding the maximizing fields of temperature and relative humidity.

Two models are developed their main difference being the parameterization of long-wave radiation. In the first, cruder model, an exponential dependence upon water vapor pathlength was assumed. In the second model, the Sasamori equations were used. In both cases, sensible heating at the surface was accounted for by the aerodynamic bulk formula. In both models all parcels were allowed to ascend the moist adiabat if they were saturated and in this way moist adiabatic processes were included.

Observations indicate an atmospheric efficiency of about 1-2%, or a rate of generation of APE of about 2-6 watts/m<sup>2</sup>. The rate of generation of MAE from a 2-level 2-latitude model using the Sasamori radiation equations, yielded a generation rate for MAE of 12.1 watts/m<sup>2</sup>. This result is very sensitive to relative humidity. The maximizing fields of temperature and relative humidity displayed several important feature found in the real atmosphere including the horizontal and vertical gradients.

Thesis advisor: Edward N. Lorenz

Title: Professor of Meteorology

TABLE OF CONTENTS

	<u>page</u>
I. Introduction	7
II. Background	
1. Summary of previous research	14
2. Concept of moist available energy: development and application	18
III. The Approach	25
IV. The Model	29
1. Water vapor pathlength	36
2. Long-wave radiation	38
3. Short-wave radiation	43
4. Small-scale flux of sensible heat	44
5. Balances and constraints	45
6. Finding the reference state	47
7. Heating	51
V. Results	
1. Group #1: approximate expression for long-wave flux	53
2. Group #2: Sasamori parameterization of long-wave flux	58
VI. Discussion of Results	63
VII. Summary and Conclusions	80
Appendix: Computation of Long-wave Radiative Fluxes	84
Acknowledgments	85
References	86

LIST OF FIGURES & TABLE

5

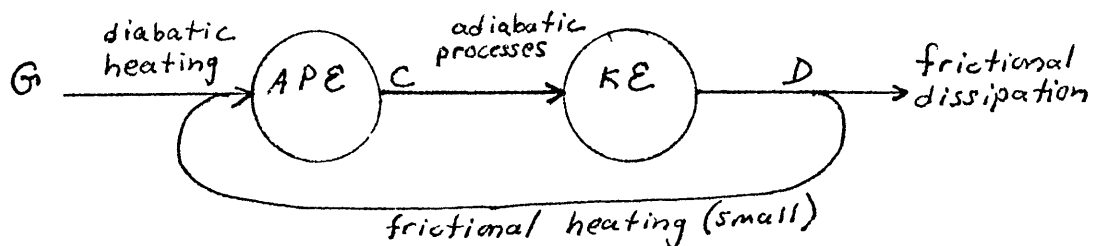
	<u>page</u>
TABLE 1. Summary of maximum rates of generation of APE by Schulman (1974)	16
 <u>FIGURE</u>	
1. Schematic of present model	12
2. MAE distribution by Wojcik (1977)	24
3. Initial T,R fields for present model	33
4. Absorption curves for water vapor after Sasamori (1968)	41
5. Maximizing T-field for R=50%	54
6. Maximizing T-field for R=90%	54
7. Maximizing T-field for R=10%	56
8. Maximizing T-field for R(4)=90%, R(1-3)=50%	56
9. Maximizing T-field for R(4)=10%, R(1-3)=50%	57
10. Maximizing T-field and R-field	57
11. Maximizing T-field for R=50% Sasamori approx.	59
12. Maximizing T-field for R(4)=10% Sasamori approx.	59
13. Maximizing T-field for R(4)=90% Sasamori approx.	60
14. Maximizing T-field and R-field for Sasamori approx.	60
15. Final maximizing T,R-fields	67
16. Zonally averaged annual mean T-field after Oort and Rasmusson (1971) for Northern Hemisphere	69
17. Latitude-height distribution of Relative Humidity for Summer & Winter after Manabe & Wetherald (1967)	71

<u>FIGURE</u>		<u>page</u>
18a.	Maximizing distribution of non-frictional heating, $Q$ .	73
18b.	Maximizing distribution of efficiency factor $N$ .	73
19.	Distribution of MAE ( $J\ kg^{-1}$ ) after Lorenz (1978)	74
20.	Observed distribution of efficiency factor, $N$ ( $10^{-2}$ ) after Newell et al (1974)	76
21.	Observed distribution of net non-frictional heating, $Q_{net}$ ( $^{\circ}k/day$ ).	77

## I. Introduction

The problem of calculating the efficiency of a moist atmosphere has long been avoided due to the intractability of moist processes. If, as in the past, the atmosphere is modelled as a heat engine, the efficiency may be defined as the ratio of energy out-put to energy input. Using this definition, Lorenz(1955) hypothesized that the atmosphere may in fact be running at near maximum efficiency.

In the case of our atmosphere, the energy input is simply the incoming solar flux incident on the outer extremity of the atmosphere. This is also called the solar constant and has been measured to be approximately 350 watts/m<sup>2</sup> of the earth's surface. By considering the energy cycle of the atmosphere, it has been found that the energy out-put may be expressed by three equivalent quantities. Following Lorenz (1955) the energy cycle may be displayed schematically:



where  $G$  = net generation of available potential energy, (APE)

$C$  = conversion of available potential energy to kinetic energy (KE)

$D$  = dissipation of kinetic energy by friction.

In the long run, when these quantities are averaged over a long time period, it may be seen that  $G=C=D$ . We express a time average as  $(\bar{\quad})$  so that in this case  $\bar{G}=\bar{C}=\bar{D}$ . Furthermore, since frictional dissipation always results in heating eg. there is no such thing as frictional cooling,  $\bar{D}$  is a positive quantity.

The energy output required to determine the efficiency, would usually be thought of as the rate of generation of kinetic energy. If, however, we consider only long time spans, we may say that the atmospheric efficiency is directly proportional to the generation rate of APE or, equivalently, to the rate of conversion of APE to KE.

In the past, attempts have been made to gain insight into the atmospheric efficiency by determining  $\bar{D}$  and  $\bar{C}$  observationally. Brunt (1926) estimated  $\bar{D}$  to be about 5 watts/m<sup>2</sup>. Unfortunately, little is known about which is the most accurate method of obtaining a value for the total frictional dissipation. One could make the assumption that most of the dissipation occurs in the lower boundary layer, so that in the Ekman solution, there is a balance between cross-gradient flow and frictional dissipation. The main problem with this method is that the frictional term must be obtained by estimating  $-g\{u \cdot \nabla z\}$  which is simply equal to  $\bar{C}$ . What we would prefer, is an independent estimate of  $\bar{D}$  so that this method is not really



desirable. Attempts have been made by Kung(1966,1967,1969) and Holopainen (1963) to determine  $\bar{D}$  indirectly as a residual term in the kinetic energy equation. The resulting values for  $\bar{D}$  were, respectively, 5.6 watts/m<sup>2</sup> and 10.4 watts/m<sup>2</sup>.

If, instead of  $\bar{D}$ , we try to evaluate  $\bar{C}$ , similar difficulties arise. Evaluation of  $\bar{C}$  requires the measurement of cross-isobar flow, which, as we have seen, is not independent of friction. Again, we would not be obtaining an independent estimate of  $\bar{C}$  if this method were used.

In light of the difficulties that arise in estimating  $\bar{C}$  and  $\bar{D}$  independently, we consider the evaluation of the generation term  $\bar{G}$ . It is well known that only a portion of the total potential energy in the atmosphere is available for conversion into kinetic energy. (Margules, 1903). This portion has been defined by Lorenz as the available potential energy. After Lorenz (1955) the APE is the amount by which the total potential energy exceeds the potential energy of the 'reference' state. The reference state is derived from the initial existing state by reversibly and adiabatically re-arranging the mass of the atmosphere to minimize the total potential energy.

The amount of KE that can be generated, is constrained by the amount of APE that can be generated. Thus, we could arrive at an estimate for the energy output by knowing the rate of generation of APE.

Because the generation of APE is only a function of the covariance of temperature and non-frictional heating (Lorenz, 1955)  $\bar{G}$  presents itself as a most likely way to determine the atmospheric efficiency.  $\bar{G}$  may be independently estimated from  $\bar{C}$  and  $\bar{D}$ . The reason for this is simply that APE is generated when warm regions are heated and cold regions are cooled; resulting in the horizontal temperature gradient required for generation of APE.

In the past, investigations of the efficiency of the atmosphere have been limited to a dry atmosphere. When we say 'dry', what is really meant is that moist processes are not considered. This does not mean that there is no relative humidity greater than zero. It simply means that the relative humidity has been held constant at some value less than 100%. Specifically, latent heat energy is not considered to be a form of internal energy which it really is. Instead, the release of latent heat is treated as a form of external or diabatic heating. More recently however, Lorenz (1978) was able to define the quantity of moist available energy (MAE), such that moist adiabatic processes may be included, along with dry ones. Unlike APE, there is, at present, no existing analytical expression for MAE or its rate of generation. Therefore, instantaneous values of  $G$  (MAE) must be obtained numerically.

The intent of this thesis is to investigate the maximum efficiency of a moist atmosphere by considering the

rate of generation of MAE in place of APE (which is equivalent to dry available potential energy, DAE). That is, we will seek the temperature and relative humidity fields which simultaneously maximize the rate of generation of MAE. To this end, we have modelled the atmosphere in such a way, that all processes may be expressed by the behavior of four parcels, each of a fixed mass. By neglecting clouds and ozone,  $G(\text{MAE})$  is reduced to a function of temperature and relative humidity distribution only. The schematics of this atmosphere may be viewed in Figure 1.

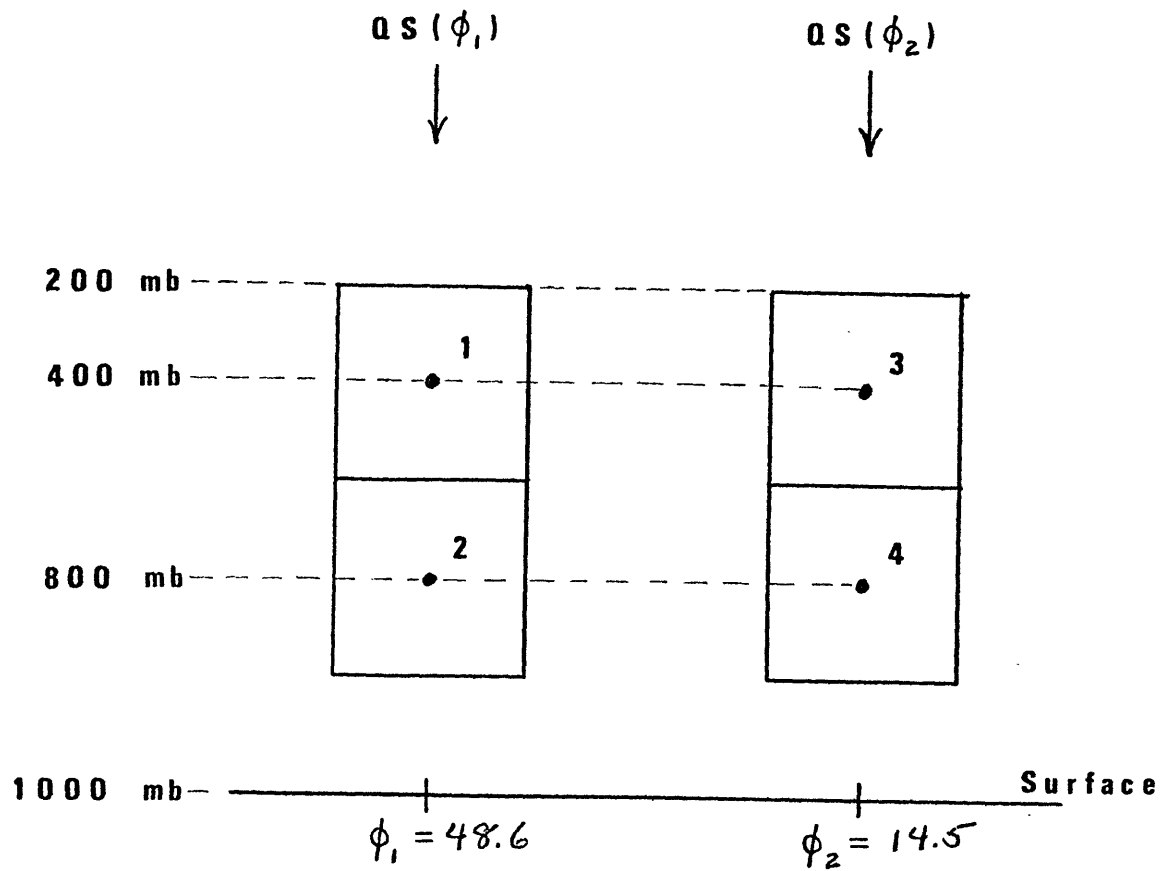
There are two ways to generate MAE:

1) diabatic heating and 2) evaporation of water vapor.

In this paper, we are considering the generation of MAE by diabatic heating only: we do not allow for evaporation.

As such, our final value for the maximum rate of generation of MAE is not as large as the value we would have gotten by including evaporation. It should be noted that the maximizing fields of temp., relative humidity, efficiency and heating would also look different if evaporation were included. The process of evaporation and precipitation are difficult to parameterize and their inclusion goes beyond the scope of this study.

Using the various estimates for the rate of generation of APE and a solar constant of  $350 \text{ watts/m}^2$ , we calculate an



$$q_s(\phi_1) = 206 \quad \text{watts/m}^2$$

$$q_s(\phi_2) = 301 \quad \text{watts/m}^2$$

Figure 1

atmospheric efficiency of about 1-2%. The estimates of G(APE) have been valued at near  $3 \text{ w/m}^2$  by Newell et al (1974),  $5.6 \text{ w/m}^2$  by Dutton and Johnson (1967) and  $2.3 \text{ w/m}^2$  by Oort (1964). Using a simple four parcel atmosphere, we have attempted to ascertain how near to maximum efficiency a moist atmosphere actually operates.

## II. Background

### 1. Summary of previous research

One of the earliest attempts at determining the atmospheric efficiency was made by Wulf and Davis (1952). Their definition of efficiency differed from the one used in this paper in that it was inversely proportional to the maximum possible frictional dissipation allowed by the observed distribution of temperature and heating. The efficiency itself was defined to be the ratio of the observed frictional dissipation to the maximum allowable dissipation. The value that resulted from this formula was 100%.

In 1955, Lorenz (1955) performed a theoretical study of the efficiency of a 'dry' atmosphere. Using a 2-dimensional model, he assumed that the rate of generation of APE was solely a function of the distribution of temperature for a given pattern of solar forcing. Water vapor was the only absorbing constituent and its mixing ratio was held constant. In addition, Lorenz used the grey approximation with all atmospheric heating due to the long-wave radiation alone. In spite of such unrealistic assumptions, he was able to conclude that the atmosphere was in fact constrained to operate near maximum efficiency.

The most recent work to date concerning the efficiency

of the atmosphere, was completed by Schulman (1974). His approach included a series of simple numerical models which increased in resolution and complexity. By imposing constraints similar to Lorenz's assumptions upon these models, the rate of generation of APE was determined solely as a function of temperature. To this end, Schulman specified the relative humidity as a constant value everywhere. He also neglected ozone and used the observed mixing ratio for carbon dioxide. The release of latent heat was treated externally as a form of diabatic heating, while water vapor, the only other absorbing medium, was allowed to vary only with temperature. The flux of sensible heat, when included, was parameterized by the aerodynamic bulk formula. Table 1 summarizes the results for the various models used. It is immediately clear that his investigation was supportive of Lorenz's hypothesis concerning the efficiency of the atmosphere.

The actual 'features' of the maximizing temperature field turned out to be quite similar to those observed in our own atmosphere. The most prominent and possibly the most important characteristic of this temperature field is the presence of a horizontal temperature gradient, the magnitude of which decreases with height above the surface. Furthermore, Schulman found that the vertical temperature gradient was largest near to the equator. Hence, the static

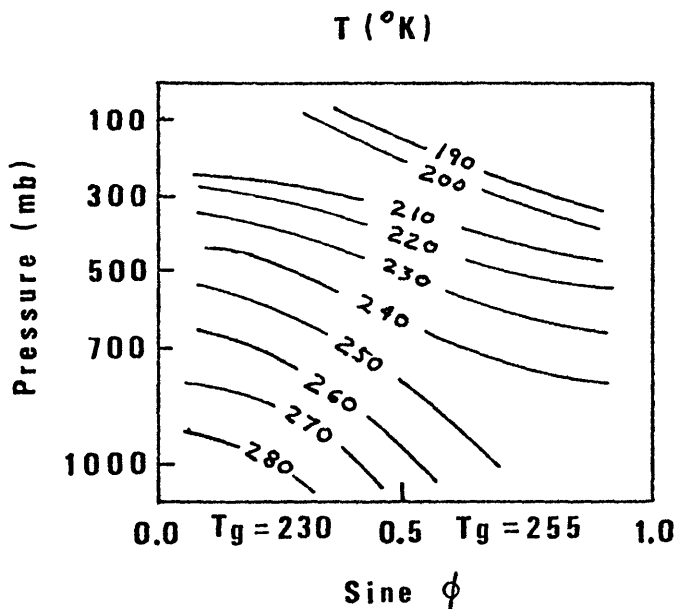
relative humidity =50%  
 albedo =30%  
 wind speed =10 m/s  
 $\delta$  =0

maximum rate of generation of APE using 3-level, 2-latitude model was  $G=5.2 \text{ watts/m}^2$  ; no sensible heating

maximum rate of generation of APE using 3-level, 2- latitude model and initial temperature field was  $G=4.1 \text{ watts/m}^2$  ; sensible heating included.

maximum rate of generation of APE using same model as above with maximizing temperature field was  $G=7.8 \text{ watts/m}^2$   
 efficiency = 2.3%

maximizing temperature distribution:





stability was largest in the high latitudes as is observed in our atmosphere. In light of the fact that the temperature distribution for which the rate of generation of APE is a maximum maintains some important likenesses to the observed temperature distribution, one could at some level, conclude that our atmosphere must be running rather close to a maximum efficiency of about 1-2%.

In order to ascertain the degree of sensitivity of the maximum, several of the model parameters were varied. Schulman found that the maximum was relatively insensitive to changes in albedo, surface wind speed and, surprisingly, relative humidity. The sensible heat scheme chosen was found to be very influential on the results. The range of maximum efficiencies for these variations went from 5% to near 3%.

To test the maximization schemes (graphical and numerical) Schulman varied his initial temperature fields. When the distribution was grossly unrealistic, the generation of APE was always negative- that is, APE was destroyed. In all cases of 'realistic' initial temperature fields, the convergence was consistently to the same maxima.

The work of Schulman described above along with the recently completed study of moist available energy by Lorenz(1978), both provided the impetus for the present investigation of the efficiency of a moist atmosphere.

2. The concept of moist available energy:  
development and applications

The incoming solar radiation heats up the atmosphere and the underlying surface of the earth to produce internal energy (IE). Motion on all scales indicates that a supply of kinetic energy (KE) exists in the atmosphere. Friction causes a continual dissipation of KE. According to Lorenz (1967), one of the main problems in the theory of the general circulation is the question of how some of the IE produced by solar heating, is converted into KE in order to maintain the motions that are observed. We know that the net longterm heating due to radiation and conduction is equal to zero while the net heating due to frictional dissipation is greater than zero and positive. In fact, the total net heating over the long run is equal to  $Q_f$ , the frictional heating.

Because of the fact that the atmosphere is approximately in hydrostatic equilibrium, certain constraints are placed upon the energy conversion processes. Specifically, it can be shown that the ratio of potential energy (PE) to internal energy is proportional to 2/5. Since PE is linearly proportional to IE, both quantities increase and decrease together and we may consider the sum IE+PE instead of each form separately. After Margules (1903), we call the sum the total potential energy (TPE). Furthermore, it is

easily shown that TPE per unit mass is equal to  $C_p T$  which is simply the sensible heat per unit mass.

Following Lorenz (1967) we may now formulate an expression for the rate of change of TPE and KE:

$$\frac{\partial (\text{TPE})}{\partial t} = H - C$$

$$\frac{\partial (\text{KE})}{\partial t} = C - D$$

where  $H = \{Q\}$  = total heating /unit mass

$D = -\{\underline{U} \cdot \underline{F}\}$  = total dissipation /unit mass

$C = -\{\omega \alpha\} = -\{g \underline{U} \cdot \underline{\nabla} z\}$  = total rate of conversion of  
KE / unit mass

$\{ \}$  = per unit mass

$(\bar{\quad})$  = averaged over long term

Unfortunately, several problems arise when one attempts to evaluate H, C, or D, directly. One possibility here is to utilize the constraint that in the long run, the heating does not change the entropy. Or:

$$\overline{\{ Q (1 - T_1/T) \}} = \bar{H}$$

Since  $ds/dt=0$  and  $T_1$  is such that  $1/T_1 = \{\bar{1}/\bar{T}\}$ , then we can estimate  $\bar{H}$ . This is plausible since, now, the errors in  $Q$  are largely cancelled by errors in  $Q(T_1/T)$ . This method was used by Lettau (1954) and yielded a value of  $\bar{H}=2 \text{ watt/m}^2$ .

In the interest of gaining more insight into the rate of generation of KE that is required to balance the frictional

dissipation, we introduce the concept of APE. APE may be best defined as the difference between TPE and the un-available potential energy. Because the conversion of TPE to KE is both reversible and adiabatic, the potential temperature of each parcel of air is preserved in such a conversion, so that the statistical distribution of  $\theta$  is also maintained. There is only one state, however, that possesses the least TPE. This state has been labelled the 'reference state'. In fact, in the reference state, the un-available potential energy is equal to the TPE by definition. If we specify the total potential energy as the sum of internal energy plus potential energy, then

$$\int (\text{TPE}) \rho dz = \int (\text{PE} + \text{IE}) \rho dz = \int (gz + C_v T) \rho dz = \int (C_p T) \rho dz = \int h \rho dz = \int \text{enthalpy} \rho dz$$

The reference state is that arrangement of mass which yields the least enthalpy. Hence  $\text{APE} = \{\bar{h}\} - \{\bar{h}\}_{\text{min}}$ .

We saw before that the net long-term production of TPE by non-frictional heating is zero since  $\{\overline{Q_n}\} = 0$ . Therefore, the net long-term production of TPE by frictional heating = the net production of TPE by all modes of heating. But, in converting KE to TPE, the frictional influence is to raise the  $\theta$  of some parcels. On the other hand,  $\theta$  is never decreased by friction. Therefore, the UPE is raised by the same amount that TPE is raised. Thus, the APE produced by friction must be less than the TPE produced. This indicates that we have a net production

of APE by heating other than friction. An estimate of the rate at which non-frictional heating generates APE will then give us information on the rate of generation of KE. Since this is proportional to the atmospheric efficiency, we gain insight into the efficiency without having to deal directly with friction.

Using the above concepts, Lorenz (1955b) derived an exact expression for APE. He then used an approximate form and formulated the rate of change of APE by:

$$\partial(APE)/\partial t = G - C$$

where:  $G = \{N Q\}$  = rate of generation of APE per unit mass  
and  $N$  = the efficiency factor = the effectiveness of

heating at any point in producing APE =

$$1 - (P_r/P)^\zeta \quad : \quad P_r = \text{reference pressure} \\ \zeta = R/c_p$$

With the approximate form of APE, Lorenz obtained a value for  $G=4$  watts/m<sup>2</sup>.

Thus far, we have considered APE to be the available energy for a dry atmosphere. That is, an atmosphere for which moist adiabatic processes are not included. Moist available energy (MAE) has been defined by Lorenz (1978) as "the amount by which the potential plus internal (including latent heat) energy of a given atmospheric mass field exceeds that of a hypothetical reference field, which can be constructed from the given field by re-arranging

the atmospheric mass under reversible dry and moist-adiabatic processes, to minimize the potential plus internal energy."

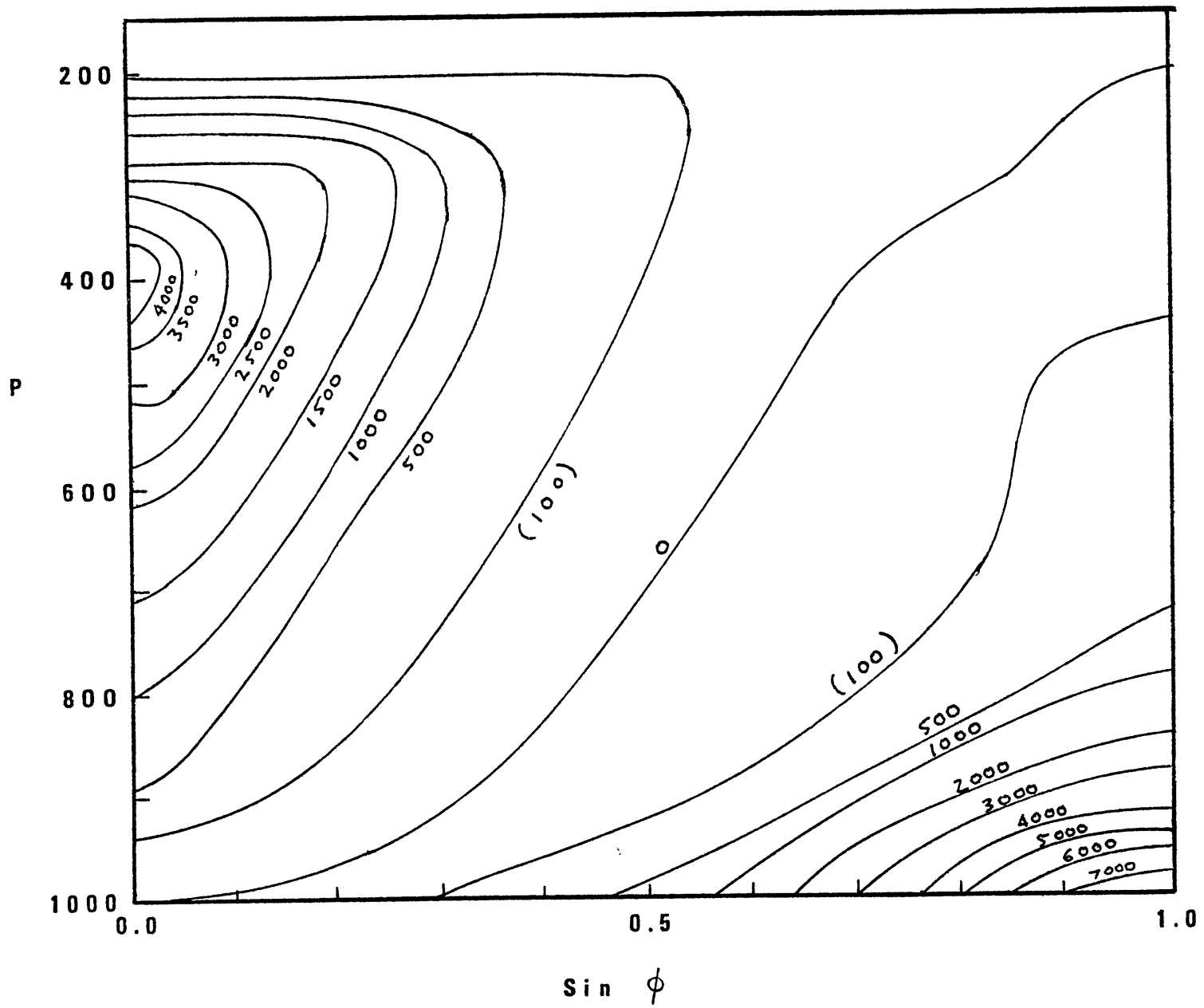
The hypothetical reference field can best be understood by the following line of reasoning. The conversion of TPE into KE is accomplished by processes that are both reversible and adiabatic. If the mass in the system is re-arranged adiabatically, then the enthalpy of the system will change in a manner opposite to the KE change. If in addition we specify that the atmosphere be in stable equilibrium after this re-arrangement, then the total enthalpy will be at a minimum, while the total KE will be at its maximum value. This defines the reference state as that arrangement of mass which yields a minimum total enthalpy and is most statically stable. The increase in KE from the initial state to the reference state is equal to the total energy (moist) that is available for conversion. It is evident that the reference state, in order to remain statically stable, must have no vertical accelerations. Hence, all isobaric surfaces must be horizontal and hydrostatic equilibrium must prevail e.g. density is horizontally stratified.

Applying the concept of the reference field to MAE, Lorenz (1978) was able to reveal some important characteristics of the field of MAE. He found that MAE was about

21% greater than APE. Because MAE can be generated by the evaporation of water as well as by radiation and conduction, Lorenz calculated the efficiency of generation of MAE by both heating and evaporation (1978). The results indicated that evaporation was at least as efficient as heating in generating MAE.

Following this investigation by Lorenz, Wojcik (1977) made a study of the sensitivity of MAE to changes in the atmospheric temperature field. He found that a 21% increase in MAE followed a 2% increase in the zonally averaged northern hemispheric temperature field. The increase that resulted in APE was only 2%. The relative humidity field was held constant during these experiments. In figure 2, we see the distribution of specific MAE following a uniform increase of 2% in the temperature field. (A reference sounding is not a state curve and is thus approximated by many short segments of state curves. The net enthalpy loss that occurs when a parcel rises or sinks to its reference pressure is called the 'specific' MAE.)

Figure 2





### III. The Approach

In order to study the generation of MAE, we must work from a model of the atmosphere. Because the rate of generation of MAE is highly dependent upon both the temperature and the relative humidity fields, this generation is also influenced by those factors which effect the temperature and relative humidity. One of the most influential factors is clearly the atmospheric motion or dynamics. We have circumvented this problem following Schulman (1974). That is, we know that the maximum possible rate of generation of MAE results from a temperature contrast less than the radiative equilibrium temperature contrast but greater than no horizontal temperature contrast at all. We get around the complexity of including atmospheric motions simply by seeking those temperature and relative humidity fields which yield the maximum rate of generation of MAE, neglecting the motions which lead to this distribution. Possibly, this is the most major assumption that we will make.

The rate of generation of MAE is also dependent upon heating (non-frictional) since the generation requires heating of the warm regions and cooling of the colder regions. We will digress briefly to show that this must be so. Consider that both  $d\theta/dt=0$  and  $ds/dt=0$ . It then follows from the definition of the entropy,  $s$ , and the

hypsothetic formula, that:

$$\{\overline{Q/T}\} = 0, \quad \{\overline{Q/\rho^k}\} = 0$$

If we limit ourselves to only the non-frictional heating,

$Q_n$ , then since  $Q = Q_n + Q_f$  and  $\{\overline{Q_n}\} = 0$

then  $\{\overline{Q_n/T}\} < 0, \quad \{\overline{Q_n/\rho^k}\} < 0$

Hence there is a positive correlation between heating and temperature.

Non-frictional heating has three main components: radiation, conduction, and the release of latent heat. We will digress again slightly in the interest of clarity concerning the latter form of 'heating'. We mentioned earlier that MAE is defined such that the release of latent heat energy is treated internally, as a transformation of energy rather than externally, as a form of heating. In addition, the processes of evaporation, and precipitation must also be parameterized. Then, the effects of convection, advection and geography would enter in making the evaluation of  $G$  (MAE) very complicated. The problem of including these processes will be handled by approaching MAE indirectly. We would like to be able to gain some insight into the generation rate of moist available energy while not having to deal with the complexities of clouds and so forth. We attempt to accomplish this in the following manner.

We begin by assuming that in our model, the atmosphere is cloudless and that the relative humidity field, though

not constant, is always less than 100%. Since there is never any liquid water, there is no condensation of water vapor and hence no release of latent heat of condensation. Our atmosphere is still considered moist, however, since we have not required that the mixing ratio be zero or constant. Furthermore, we have included moist adiabatic processes in defining the reference field.

In assuming a cloudless atmosphere, we have also simplified the calculations of radiative heating, because the clouds would have reflected some incoming solar, short-wave radiation. Similarly clouds would absorb the long-wave radiation. Further simplifications result when we assume that 1) there is no ozone content, 2) there is a constant (observed) mixing ratio for carbon dioxide, and 3) water vapor is the only other absorbing constituent in the atmosphere. We also will assume that the planetary albedo is constant at 30% everywhere.

When these (and other) approximations are made, along with the requirements concerning the energetics of the atmosphere, we can determine the rate of generation of MAE by the temperature and relative humidity fields alone for a given distribution of solar forcing.

The model that we have used is essentially composed of four points or parcels of a fixed mass. We consider two different latitudes, one at  $48.6^\circ$  N the other at  $14.5^\circ$  N.

These latitudes were chosen since  $\sin(48.6) = .75$  and  $\sin(14.5) = .25$ , so that each latitude is representative of half the hemisphere. At each latitude there is one parcel at 800 mb and another aloft at 400 mb. The parcels are numbered so that parcels #1 and 3 are at 400 mb but at different latitudes while parcels #2 and 4 are similarly at 800 mb. The fields of temperature and relative humidity may be thought of as mean fields with respect to longitude. That is, we are not concerned with any longitudinal variations due to topography or land-sea contrasts. In addition, we have assumed that the solar forcing is independent of longitude as well, so that the resulting efficiency is also not a function of longitude. In reality of course, atmospheric dynamics require the existence of motions which vary with longitude so that we often observe strong gradients of temperature and relative humidity in a given latitude circle. Hence, our efficiency is constrained to always be near a maximum not necessarily exactly at it. Our zonal averaging will actually lead us to a larger value of G since MAE may be destroyed at some location on a latitude circle. In the present study, the maximizing fields are 2-dimensional, recognizing that the resulting rate of generation of MAE is higher than if we had not considered zonally averaged fields.

#### IV. The Model

In his paper on dry available energy, Lorenz (1955a) was able to derive exact analytical expressions for APE and the rate of change of APE. The rate of generation that follows from the expressions for APE is:

$$G = \int_m Q N dm, \quad m = \text{mass}$$

where  $G$  = rate of generation of APE per unit area of the earth's surface and  $N$  = efficiency factor. Lorenz set  $N = 1 - (p_r/p)^k$  where  $p_r$  = reference pressure but other forms of  $N$  have been used in the past (Newell et al., 1974).

The present 'state of the art' of MAE is such that it may only be determined graphically or numerically for a given sounding. The graphical method, used by Wojcik (1977) to determine the sensitivity of MAE to the temperature field, was devised by Lorenz (1978). He utilized this method with some success to determine the efficiency of heating (cooling) and evaporation (precipitation) in generating MAE. However, this graphical method is time consuming and, because of its very nature, the results it produces are only as good as the person performing the evaluation.

More recently, Lorenz made further investigations by using a numerical ordering scheme devised by Colman (1978). The basis of this scheme is used to obtain the reference

state in the present study. Because the work has proceeded numerically, a fast and accurate expression for the rate of generation of MAE was needed. Due to the lack of any analytical formula for MAE, we have simply used the same equation that was used for a dry atmosphere, and modified it for our purposes. Our working equation is thus:

$$G = \int_m Q N dm$$

but now  $N = 1 - (T_r/T)$  where  $T_r$  = the reference temperature. In addition,  $Q$  is now equal to the total non-frictional heating and does not include any heating due to the release of latent heat energy. In this way, we are treating latent heat release as a transformation of internal energy and not as another form of diabatic heating as has been done in the past.

If we assume that hemispherical symmetry prevails, then we may write our expression as:

$$G = \int_0^{p_0} \int_0^{1/2} \frac{1}{g} Q N \cos \phi d\phi dp$$

$p$  = surface pressure = 1000mb

$\phi$  = latitude

Following Schulman (1974), we define  $s = \sin \phi$  so that:

$$G = \int_0^{p_0} \int_0^1 \frac{1}{g} Q N ds dp$$

is the final form for the rate of generation of MAE.

In the previous section, we made some assumptions

which allowed us to neglect atmospheric motions. Further assumptions must be made in addition to these to make our task more tractable. In the interest of simplicity, we will disregard all topography and assume a smooth, uniform earth. The surface will not be allowed to store any heat so that a flux balance must be maintained at each individual latitude. The grey approximation has been assumed so that the atmosphere is transparent to all short-wave flux and the ground absorbs all the incident solar radiation. As we have chosen to neglect clouds, the atmosphere is assumed to be non-scattering as well.

The net non-frictional heating,  $Q$ , may be divided into three components:  $A = Q_{sw} + Q_{lw} + Q_{sh}$ .  $Q_{sw}$  represents the incident short-wave radiation from the sun.  $Q_{lw}$  is the long-wave radiation emitted by the ground and the parcels in the atmosphere. We have assumed that only  $Q_{lw}$  can actually heat the atmosphere. Finally,  $Q_{sh}$  is the term which represents sensible heat flux from the surface upwards. We mentioned earlier that vertical motions are not being considered in this study. Hence, the inclusion of sensible heat flux is only approximate. That is, we have parameterized the flux of heat only in the layer just above the surface. In this way, the flux of sensible heat will only come into play when we evaluate the ground temperature and impose the flux balance at a given latitude. At the 800 and 400 mb levels, the flux of heat due to

turbulent eddies is not accounted for.

In our expression for the rate of generation of MAE, we note the presence of a heating term,  $Q$ . This  $Q$  is not the sum of the three heating terms mentioned above. The reason for this is that MAE is generated in regions where there is heating or cooling. We have assumed, however, that the atmosphere is heated solely by the long-wave radiation and sensible heating at the surface. Therefore, the  $Q$  term in the equation for the generation of MAE is equal to  $Q_{lw} + Q_{sh}$ .

Because  $G$  is calculated for each parcel separately, and for many different temperature and relative humidity fields, a rapid evaluation of  $Q$  was necessary. In the interest of speed a numerical scheme was followed to estimate the radiational heating, the details of which will be described in the following sections. Before the actual steps of the method used are considered, we will present a schematic summary of the model.

Figure 3 is a representation of our hypothetical moist atmosphere. The parcels are divided up between two latitudes, with the specified pressure levels being 400 and 800 mbs. Because of the constraints of global radiative heating and surface flux balance, we cannot choose the temperature field arbitrarily. That is, given an initial temperature distribution, we must then adjust the values so that our constraints are satisfied. Once we are given the initial values of temperature and relative humidity for the



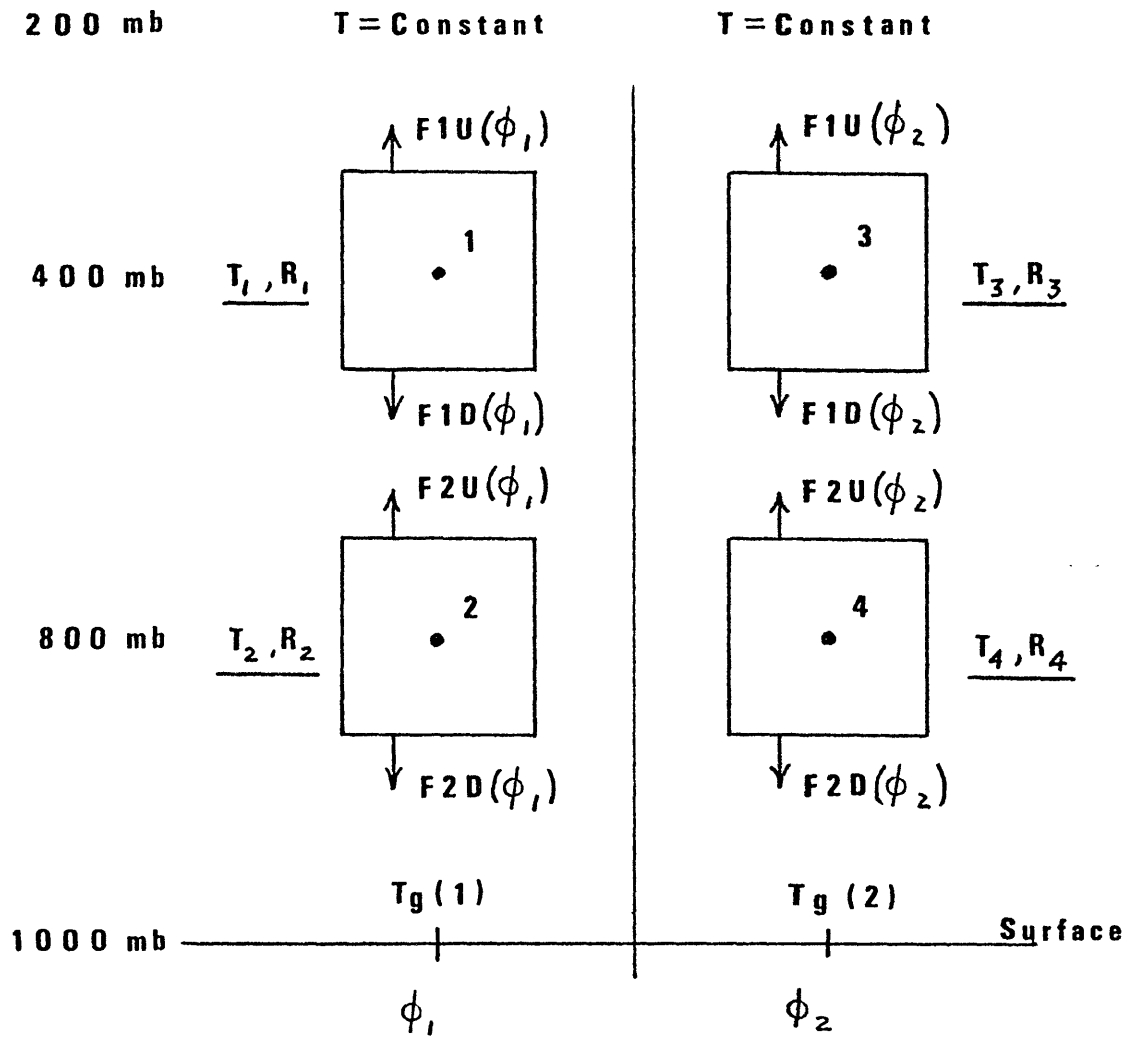


Figure 3

four parcels, we are ready to begin the search for the temperature and relative humidity distributions that maximize the rate of generation of MAE. Clearly, the first step is to decide on the initial values. These were evaluated in the following manner. Let us define a set of four variables  $V_1, V_2, V_3, V_4$ , as;

$$V_1 = T_1 + T_2 + T_3 + T_4 = 1000$$

$$V_2 = (T_1 + T_2) - (T_3 + T_4) = \text{horizontal temperature gradient}$$

$$V_3 = (T_1 - T_2) + (T_3 - T_4) = \text{vertical temperature gradient}$$

$$V_4 = (T_1 + T_4) - (T_2 + T_3)$$

Because we would like to begin with some fairly realistic temperatures, we arbitrarily decide on upper and lower limits for the variables. In this case we set the boundaries such that:

$$-150 \leq V_2 \leq 50$$

$$-150 \leq V_3 \leq 50$$

$$-100 \leq V_4 \leq 100$$

We now have four equations with four unknowns which may be rewritten as:

$$T_1 = 1/4 (V_1 + V_2 + V_3 + V_4)$$

$$T_2 = 1/4 (V_1 + V_2 - V_3 - V_4)$$

$$T_3 = 1/4 (V_1 - V_2 + V_3 - V_4)$$

$$T_4 = 1/4 (V_1 - V_2 - V_3 + V_4)$$

If, for the moment, we concern ourselves solely with the temperature field, we can see that there are 125 different

temperature profiles as the variables run from their lower to their upper limits, in increments of 50. If  $V_1$  were variable, we would have 625 different grid points, but we have fixed  $V_1$  initially for simplicity. We can view this as a  $5 \times 5 \times 5$  grid where each grid point represents a different temperature distribution. Hence, for each grid point, there is a rate of generation of MAE. The idea here is to search this grid for the largest value of  $G$ . Then, by making the increments successively smaller, we will hopefully arrive at that point whose temperature distribution yields the largest rate of generation. We proceed in a similar fashion with the field of relative humidity. Now however, the relative humidity of each parcel may only vary from 10 to 90%. As with the temperature field, we end up with four equations:

$$R_1 = 1/4 (z_1 + z_2 + z_3 + z_4)$$

$$R_2 = 1/4 (z_1 + z_2 - z_3 - z_4)$$

$$R_3 = 1/4 (z_1 - z_2 + z_3 - z_4)$$

$$R_4 = 1/4 (z_1 - z_2 - z_3 + z_4)$$

where;  $z_1 = 2.0$

$$-1.2 < z_2 < .8, \quad -1.4 < z_3 < .4$$

$$-.4 < z_4 < 1.4$$

The grid is no longer a simple  $5 \times 5 \times 5$  array when we include a variable relative humidity. Now, there are six dimensions instead of three, because we seek the temperature

and relative humidity fields which simultaneously maximize G.

Once we have decided on our initial eight values, the balances which constrain these fields must be imposed in order to obtain the final working fields. To this end, we must evaluate the fluxes that enter into the balance requirements.

### 1. Water vapor pathlength

In order to determine the long-wave fluxes we not only need to know the temperature and relative humidity of each parcel, but the water vapor pathlength as well. The exact dependency of long-wave radiation upon the pathlength of water vapor will be discussed in the next section.

Using the basic thermodynamic equations for the atmosphere, the water vapor pathlength,  $u$ , can be easily derived. Given the temperature of each of the four parcels,  $T_1, T_2, T_3, T_4$ , we can determine the saturation water vapor pressure as:

$$e_s(T) = 6.11 \left( \frac{273.16}{T} \right)^{5.0065} \times \exp \left[ 24.84 \left( 1 - \frac{273.16}{T} \right) \right]$$

Then with the given relative humidities, the water vapor mixing ratio is:

$$q(P, T, R) = R \left[ .622 \times e_s(T) / (P - e_s(T)) \right]$$

The water vapor pathlength is measured from the top of the atmosphere downward to some level  $p$  in a column of unit cross-sectional area, and may be expressed by:

$$u(P, T, R) = \frac{1}{g} \int_0^P q \frac{p}{p_0} dp$$

This equation is valid as long as we assume that the width of the absorption lines changes linearly with pressure. If we let  $P = p/p_0$  where  $p_0 =$  the surface pressure, and assume that  $q$  varies exponentially from  $P$  to  $P+\Delta P$ , then we may write:

$$q = q_0 P^m \quad \text{where, for } \Delta P = P_2 - P_1, P_2 > P_1$$

$$q_0 = \frac{q_2}{P_2^m}, \quad m = \frac{\log [q_2/q_1]}{\log [P_2/P_1]}$$

Substituting into our equation for  $u(P, T, R)$

$$u(P_2) - u(P_1) = \frac{P_0}{g} q_0 \int_{P_1}^{P_2} P^{m+1} dp$$

$$\text{or: } u(P_2) = u(P_1) + \frac{P_0 q_0}{g} \frac{1}{(m+2)} \left[ P_2^{m+2} - P_1^{m+2} \right] \left( \frac{gm}{cm^2} \right)$$

and  $P_0/g =$  total mass in a column of unit cross-sectional area.

The upper boundary to our model atmosphere is assumed to be at 200 mb where we have assumed a constant water vapor mixing ratio. For  $p = 200$  mb,

$$u(200\text{mb}) = .005 \frac{P_0}{g} \int_{200} g \quad (\text{gm/cm}^2)$$

To account for the absorption due to carbon dioxide, we must calculate the pathlength of CO<sub>2</sub> as well. As mentioned before we handle the contribution of CO<sub>2</sub> by using the observed mixing ratio and assuming that it is constant throughout the atmosphere. This being the case, the CO<sub>2</sub> pathlength is formulated as:

$$u_c(p) = 0.5 \frac{P_0}{g} g_c \left(\frac{p}{P_0}\right)^2 \quad (\text{gm/cm}^2)$$

## 2. Longwave Radiation

Two different parameterizations were used to model the longwave radiation. The first, and simplest, was implemented because we wished to reduce the complexity of the numerics in order to get the model working. The basic assumption here was that the longwave flux varied exponentially with the water vapor pathlength. For example, the downward flux across parcel number 2 was determined to be:

$$F_{\downarrow}(2) = \sigma T_2^4 (1 - e^{-au_2}) + \sigma T_1^4 (1 - e^{-au_1}) e^{-au_2}$$

where 'a' was a proportionality constant that was arbitrarily chosen to equal the reciprocal of some typical water vapor pathlength. Because we assumed that the thermodynamic properties of each parcel were uniform

throughout a given parcel, we concluded that the longwave flux from that parcel would be expressed by  $\sigma T^4(1 - e^{-au})$  and that the radiation was equal and opposite in both directions. This of course is a very crude approximation for the longwave flux and not unexpectedly produced results that were not very realistic. Once the numerical model was working, the longwave fluxes were re-parameterized using the Sasamori equations.

Sasamori (1968) found that the absorption functions of water vapor and carbon dioxide in Yamamoto's radiation charts (1952) could be written as empirical expressions. Hence, for a cloudless atmosphere, the longwave flux formulae are:

$$F_{\downarrow}(p) = 4\sigma \int_0^{T(p)} \bar{A} \{u(T'), T'\} T'^3 dT'$$

$$F_{\uparrow}(p) = \sigma T_g^4 + 4\sigma \int_{T(p)}^{T(\rho)} \bar{A} \{u(T'), T'\} T'^3 dT'$$

where  $\bar{A}(u, T)$  is the normalized absorptivity and may be expressed by:

$$\frac{R(u, T)}{4\sigma T^3} = \frac{\int_0^{\infty} [1 - \tau_f] \frac{dB_{\nu}}{dT} d\nu}{\int_0^{\infty} \frac{dB_{\nu}}{dT} d\nu} ; \quad \text{where } R(u, T) = \text{mean absorptivity} = \int_0^{\infty} [1 - \tau_f] \frac{dB_{\nu}}{dT} d\nu$$

$\tau_f$  = mean transmissivity,  $B_{\nu}$  = Planck's function,  $T_g$  = ground temperature. The layer between 1013 and 1000 mb is assumed to be transparent and contributes no flux.

Sasamori found that the mean absorptivity is approximately constant with temperature between about 200-300°K as may be seen in figure 4. That is, in this range of temperature, the 6.3  $\mu$  bands have the same intensity as the rotational bands. At very low temperatures, only the rotational bands contribute to the absorptivity so that the mean absorptivity increases with decreasing temperature. If the level  $P_1$  is the level above which the pathlength changes very little, then the downward flux may be written as:

$$F_{\downarrow}(p) = 4\sigma \int_{T(p)}^{T(p_1)} \bar{A}_0 \{u(T') - u(T(p))\} T'^3 dT' + \sigma T(p_1)^4 \bar{A} \{u(T(p_1)) - u(T(p)), T(p_1)\}$$

since the difference  $u(T(p_1)) - u(T(p))$  is approximately constant from  $p=0$  to  $p=p_1$ .

From  $p=p_1$  to  $p$ ,  $\bar{A}(u, T')$  can be approximated by  $\bar{A}_0(u)$  so that the absorptivity is no longer a function of  $T'$ . In this particular study, we have not considered any downward longwave flux from the top of the atmosphere, so that we formulate the downward flux at some level  $p$  as:

$$F_{\downarrow}(p) = 4\sigma \int_{T(p)}^{T(p_1)} \bar{A}_0 \{u(T') - u(T(p))\} T'^3 dT'$$

Specifically, we regard the 200 mb level as our upper boundary, assuming that the atmosphere above this level is transparent. Thus, no radiation is absorbed by this region



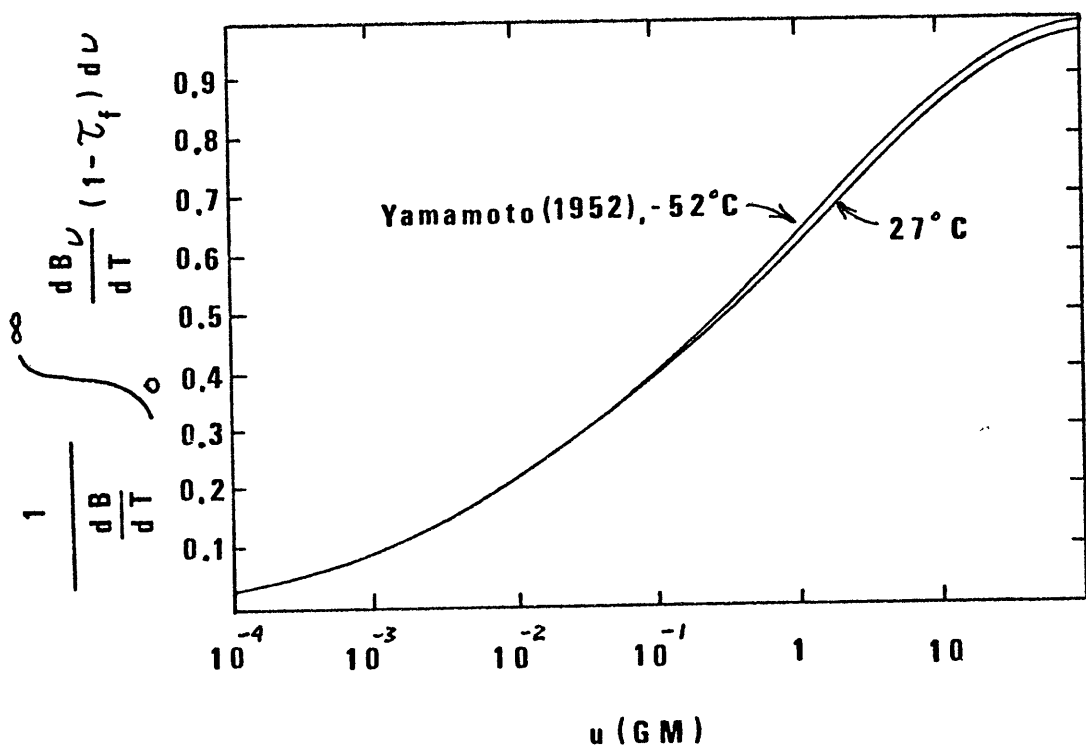


Figure 4

and it cannot contribute at all to the net longwave flux.

The new absorptivity functions were expressed by Sasamori as:

$$\bar{A}_0(u) = \bar{A}_w(u_w) + \tau_w \bar{A}_c(u_c)$$

where  $\bar{A}_w$  = absorptivity function for water vapor

$\bar{A}_c$  = absorptivity function for carbon dioxide

$\tau_w$  = correction factor due to overlap of water vapor

and carbon dioxide curve near  $15\mu$ . = transmissivity

The empirical expressions for the above are :

$$\bar{A}_w = 0.846 (u_w + 3.59 \cdot 10^{-5})^{0.2+3} - 0.0690 = \bar{A}_{w1}; \quad u_w < 0.01 \frac{\text{gm}}{\text{cm}^2}$$

$$\bar{A}_w = 0.240 \log(u_w + 0.010) + 0.622 = \bar{A}_{w2}; \quad u_w > 0.01 \frac{\text{gm}}{\text{cm}^2}$$

Schulman (1974) found that a discontinuity in the first derivative of  $\bar{A}_w$  existed for  $U_w = 0.01 \text{ gm/cm}^2$ . He suggested that the two expressions for  $\bar{A}_w$  be combined to yield:

$$\bar{A}_w = \bar{A}_{w2} + (\bar{A}_{w1} - \bar{A}_{w2}) \exp^{-[6931.5 u_w^2]}$$

which is valid for all  $U_w$  and is continuous. The Sasamori empirical fit for the  $\text{CO}_2$  absorption curve is:

$$\bar{A}_c = 0.0546 \log u_c + 0.0581$$

while the transmissivity of water vapor was best fit by:

$$\tau_w = 1.33 - 0.832 (u_w + 0.0286)^{0.260}$$

Using these empirical formulae, the final working expressions for the longwave flux were found to be:

$$F_{\downarrow}(p) = 4\sigma \int_{T(p)}^{T(p)} \bar{A}_0 \{u(T') - u(T(p))\} T'^3 dT'$$

$$F_{\uparrow}(p) = \sigma T_g^4 + 4\sigma \int_{T(p_0)}^{T(p)} \bar{A}_0 \{u(T(p)) - u(T')\} T'^3 dT'$$

These flux equations are valid for temperatures between just below 200°K and just above 320°K.

The rate of atmospheric heating due to longwave radiation is formulated by:

$$Q_L(p) = g \partial [F_L(p)] / \partial p$$

where  $F_L(p) = F_{\uparrow}(p) - F_{\downarrow}(p)$

= net longwave flux at a level p.

See Appendix for more detailed calculation of long-wave fluxes.

### 3. Shortwave Radiation

In this model all incident shortwave radiation is absorbed by the ground so that the atmosphere is transparent to all incoming solar radiation. After the solar radiation is reflected by the top of the atmosphere and the surface, the amount remaining that is available to be absorbed by the ground is:

$$F_{sw}(s) = F_s(s) [1 - \alpha]$$

where  $s = \sin \phi$  and  $F_s(s) = S_0 \overline{\cos Z}$  = incident solar flux before reflection.

$S$  = solar constant = 1395 watts/m<sup>2</sup>

$L$  = fraction of a 24 hour day that the sun is above the horizon.

$z$  = zenith angle of the sun

$\delta$  = solar declination = 0 so that

$$\cos Z = \cos \phi \cos \beta \quad \text{where } \beta = \text{hour angle}$$

Although we have assumed that only the longwave flux may heat the atmosphere, we still must use the above in order to estimate the incoming shortwave radiation for the balance constraints.

#### 4. Small scale flux of sensible heat

Because of our assumption that no heat is stored or transported within the surface, we are required to account for the vertical flux of sensible heat at the surface. An often used parameterization for this quantity is the aerodynamic bulk formula:

$$F_{SH}(s) = \rho_g C_p V_o (T_g - T(p))$$

where  $\rho_g$  = air density at 1000 mb

$C_p$  = specific heat of air at constant pressure

$C_D$  = drag coefficient empirically estimated by Kraus (1972) to be =  $1.3 \times 10^{-3}$

$V_o$  = wind speed at the anemometer level = 10m/sec

We have considered the sensible heating at the ground but for the sake of simplicity we have not included the

the turbulent flux of sensible heat at higher levels in the atmosphere. As such, we include sensible heating only to the extent that the net flux of longwave radiation from the ground is:

$$F \uparrow(s)_{\text{ground}} = \sigma T_g^4 + F_{\text{SH}}(s)$$

It should be noted however, that all of  $F_{\text{SH}}(s)$  is absorbed while only a portion of  $\sigma T_g^4$  is absorbed. As such, we may define the net upward flux from the ground as

$$F_{\text{net}} \uparrow(s) = \text{longwave upward flux} + \text{sensible heat flux.}$$

It can be seen that the sensible heat flux influences the ground temperature, but it will not affect the heating of the upper parcels or the net longwave flux into space. In the next section we will see that this flux plays an important role in satisfying the requirement of a flux balance at the ground and subsequently determines to a large extent, the ground temperature at each latitude.

## 5. Balances and constraints

Once the initial four temperatures have been determined, they must be adjusted so that two basic constraints are satisfied. The first constraint is that a flux balance must exist at the surface for each latitude. In the terms of our model this means that:

$$F_g(\phi) \uparrow + F_{\text{SH}} \uparrow(\phi) = F_{\text{sw}}(\phi) + F_2 \downarrow(\phi)$$

where  $F_{2D}(\phi)$  = longwave flux downward through parcel #2 or #4 depending on which latitude one is at. This is simply a statement that in each latitude there must be radiative equilibrium between that ground and the atmosphere.

Secondly, we require global radiative equilibrium with space. Because of this, there can be no net heating of the atmosphere as a whole. This constraint can be expressed by:

$$\int_m Q dm = 0 \Rightarrow F_{1U}(\phi_1) + F_{1U}(\phi_2) = F_{sw}(\phi_1) + F_{sw}(\phi_2)$$

The implications of the above described balances will now be discussed in greater detail.

The requirement of a surface flux balance largely determines the ground temperature at each latitude. Given the initial four temperatures, there is only one value of  $T_g(\phi)$  that will satisfy the surface flux balance. Hence, we search for the value of  $T_g(\phi)$  for which:

$$\sigma T_g^4(\phi) + F_{sH}(\phi) - [F_{sw}(\phi) + F_{2D}(\phi)] = 0$$

Because  $T_g(\phi)$  enters into both the flux of sensible heat (through the bulk aerodynamic formula) and  $F_g^\uparrow(\phi)$ , the longwave flux upward from the ground ( $\sigma T_g^4$ ), it was necessary to use a convergence routine to arrive at the correct value of  $T_g(\phi)$ .

If  $T_g^k(\phi)$  is the  $k^{\text{th}}$  value of  $T_g(\phi)$ , then,

$$z(k) = F_{sw}(\phi) + F_{2D}(\phi) - \sigma T_g^k(\phi)^4 - F_{SH}(k, \phi)$$

and

$$T_g^{k+1}(\phi) = T_g^k(\phi) - z(k) \left\{ \frac{T_g^k(\phi) - T_g^{k-1}(\phi)}{z(k) - z(k-1)} \right\}$$

Again, the small scale flux of sensible heat was not considered in any of the layers above the surface.

Once the appropriate ground temperatures have been determined, the second constraint of no net heating is imposed. As in the case of determining the ground temperatures, a convergence scheme was used in order to find that temperature profile for which the atmosphere is in global radiation equilibrium with space.

At this point in the model, the final working temperatures plus the two ground temperatures have been obtained from the initial four temperatures. Using the final temperature distribution, and the initial field of relative humidity, the reference state of the system must now be sought.

## 6. Finding the reference state

In section II2, a working definition of the reference state was given. We now require certain information about that state in order to find the temperature and relative humidity fields that maximize the rate of generation of

MAE. Recall that the reference state is that state which has the least enthalpy and is most statically stable. Hence, we seek that arrangement of the four parcels which is most stable and for which the total enthalpy is minimized. Note please, that the method used is only suggested in the cases where the number of parcels is four or less. The reason for this will become apparent as the method is described.

We begin with the four parcels arranged in their initial positions, each with the final temperature and relative humidity, as shown below.

400	1. $T_f^1, R^1$	3. $T_f^3, R^3$
800	2. $T_f^2, R^2$	4. $T_f^4, R^4$
1000 <sub>mb</sub>	1 $\phi_1$	1 $\phi_2$

Since there are only four parcels, there are only 24 possible arrangements of these parcels in the vertical. The vertical pressure levels chosen were 300, 500, 700, 900 mbs. Hence, we examine the various permutations of positions, for example:

300	1	2	2	2
500	2	1	3	3
700	3	3	1	4
900	4	4	4	1



and so on. In this process, mass is conserved and all parcels are moved adiabatically upward or downward. The relative humidity is not held constant, and moist adiabatic lifting has been included. In each of the 24 possible permutations, the following calculations were performed.

Using the initial temperature, pressure and relative humidity, the saturation vapor pressure was determined for each parcel, before it was moved. Then, the dewpoint and potential temperature,  $T_d$  and  $\theta$ , were obtained using the hypsometric equation:

$$\theta = T_i \left( P_0 / P_i \right)^{1/\gamma} \quad \text{where } T_i, P_i = \text{initial pressure and temperature}$$

and the approximate equation:

$$T_d = 1.0 / \left\{ \left( 1 / 273.16 \right) - \left( 1.844 \cdot 10^{-4} \right) \ln \left[ R \times e_s(T) / 6.11 \right] \right\}$$

The above quantities were then used to estimate the LCL (level of condensation) for each of the four parcels.

That is, the temperature and pressure at the LCL were found from:

$$T_c = T_d - \left( 0.001296 \times T_d - 0.15772 \right) (T_i - T_d)$$

$$P_c = 1000 \left( T_c / \theta \right)^{3.4965}$$

Once  $P_c$  was found, we then asked if  $P_c$  was less than or greater than the pressure to which the parcel would be adiabatically moved ( $P_n$ ). If  $P_c < P_n$ , then the parcel

could be moved dry adiabatically to its new location. Since  $\theta$  is conserved along an adiabat, the final temperature for this parcel was calculated from:

$$T_f = \theta \left( \frac{P_n}{P_0} \right)^{\kappa} \quad ; \quad \kappa = R/c_v$$

The next step was to determine the specific humidity using:

$$g = R \times .622 \left[ \frac{e_s(T_i)}{P_0} - e_s(T_i) \right]$$

In the dry case, the specific humidity would not change from the initial to the final position.

If, on the other hand,  $P_n < P_c$ , moist processes must be accounted for. This being the case, the parcel was taken up the dry adiabat to the LCL and then along the moist adiabat from  $P_{LCL}$  to  $P_n$ . The temperature at  $P_n$ ,  $T_f$ , was determined numerically using a pseudo-adiabatic scheme devised by NWS. Once again, when the final temperature for the parcel is found,  $e_s(T_f)$ , the saturation vapor pressure, is re-calculated for  $T_f$  and is used to find the final value for the specific humidity:

$$g = .622 \left[ \frac{e_s(T_f)}{P_n} - e_s(T_f) \right]$$

where  $R = 1.0$  since the parcel is now saturated. When  $T_f$  for each parcel has been obtained for a given arrangement of the parcels, the enthalpy is then estimated from:

$$E_{NT} = \left[ C_p \sum_{i=1}^4 T_f^i + L \sum_{i=1}^4 g_i \right] \frac{\Delta P}{g}$$

$g$  = acceleration of gravity

$C_p$  = specific heat of air

$L$  = latent heat of condensation and is  $\sim$  constant

Using the above sequence of steps, the enthalpy is calculated 24 times, once for each of the 24 possible arrangements of the parcels. That ordering which yields the smallest enthalpy is then chosen as the reference state. Clearly, if there were five parcels instead of four, we would have to estimate the enthalpy 120 times. In such a case where the number of parcels  $> 4$ , this method would not be a desirable one to use.

Remembering that the rate of generation of MAE is directly proportional to the non-frictional heating,  $Q$ , one more term remains to be discussed.

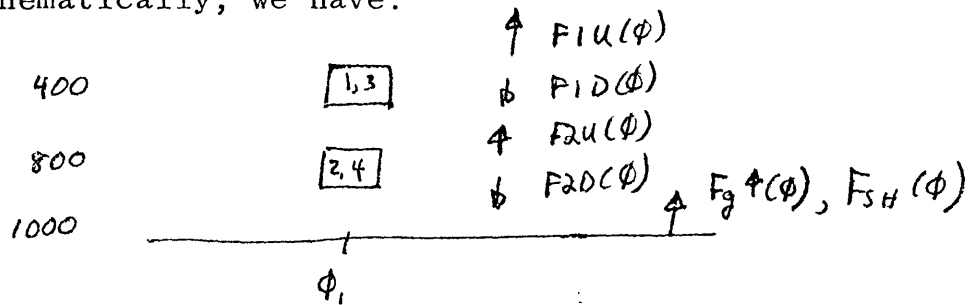
## 7. Heating

As was stated previously, the only means for heating the atmosphere in this model is through the longwave flux and sensible heat at the surface. Thus the heating may be determined from:

$$Q(\rho) = g/\Delta\rho \times \text{flux divergence}(\rho)$$

The flux divergence is determined in the following manner.

Schematically, we have:



so that the heating for the two parcels is:

$$Q(1,3) = [F_{2U}(\phi) - F_{1D}(\phi)] - F_{1U}(\phi)$$

$$Q(2,4) = [\sigma T_g^4(\phi) + F_{SH}(\phi)] - F_{2D}(\phi) - [F_{2U}(\phi) - F_{1D}(\phi)]$$

We now have evaluated the heating and temperature and reference temperature for each parcel. Using the expression for the generation of MAE:

$$G(p) = \frac{\Delta p}{g} \times Q(p) \left[ 1 - T_r(p)/T(p) \right]$$

we may determine the total rate of generation of MAE from:

$$G_{TOTAL} = \sum_{i=1}^4 G_i$$

At this point, we have a value of  $G$  for all the different temperature and relative humidity fields and we select the maximum. We now examine the temperature and relative humidity distributions responsible for this particular value of  $G$ .

## V. Results

The results may be divided into two groups. The first group was obtained using an exponential dependence for the long-wave flux, while the second group was generated using Sasamori's equations.

### 1. Group #1; approximate expression for long-wave flux

The investigation began by first letting only the temperature vary. Figure 5 is a plot of that distribution which maximized the rate of generation of MAE. This time the relative humidity was held constant everywhere at 50%. The maximum value of  $G = 31.4 \text{ watts/m}^2$ . Note that this value requires that  $T_3 > T_6$ . This was an unexpected result and was attributed to the crudity of the parameterization of long-wave flux. The efficiency of the atmosphere for this particular value of  $G$  was 9.20%.

Figure 6 is identical to figure 5 except that now the relative humidity is held constant at 90%. Similarly figure 7 is for the case where the relative humidity is set to 10%. Figures 6 and 7 simply display the sensitivity of the model to a uniform change in the relative humidity.

In figure 6 as in figure 5, we again note the inversion above 800 mb at the equatorward latitude. The generation rate however, has increased considerably to  $G = 54.1 \text{ watts/m}^2$ .

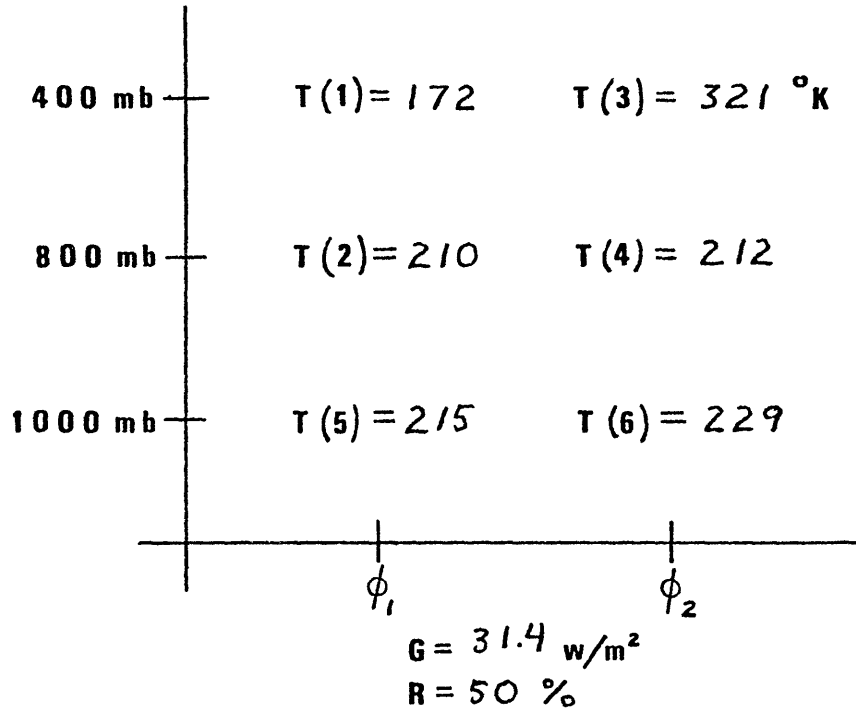


Figure 5

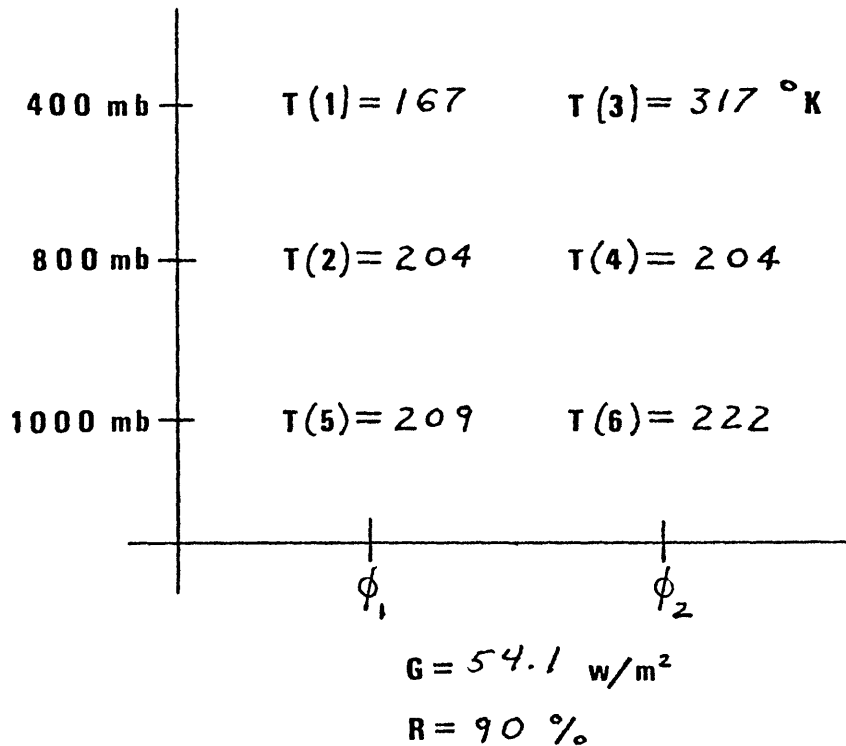


Figure 6

In figure 7 the rate of generation decreased to 15.4 watts/m<sup>2</sup>. Clearly, the rate of generation of MAE is highly sensitive to changes in the relative humidity. It is of interest to note that when Schulman tested his dry model of the atmosphere, he found that changes in the field of relative humidity did not appreciably change the rate of generation of APE.

Figures 8 and 9 represent the results for R(4) = 90% and 10% respectively. In this case the relative humidity of all other parcels is held at 50%. From the figures, it is evident that changes in the relative humidity of parcel #4 do not significantly change the rate of generation of MAE. This is due to the fact that the temperature of parcel #4 is so low that the air is nearly dry. Hence, a change in R(4) will not alter the water vapor pathlength very much. For the former value of R(4),  $G = 31.4$  watts/m<sup>2</sup> and for the latter value,  $G = 28.4$  watts/m<sup>2</sup>. The temperature profiles responsible for these values are nearly identical to each other and are quite similar to the profile in figure 5 as well.

Figure 10 is possibly the most meaningful of the results in group #1. This time, the relative humidity was allowed to vary from 10% to 90% for parcel #3, and from 10% - 50% for parcel #4. We can see that the temperature profile which, along with a certain field of relative humidity, maximizes the rate of generation of MAE, is not

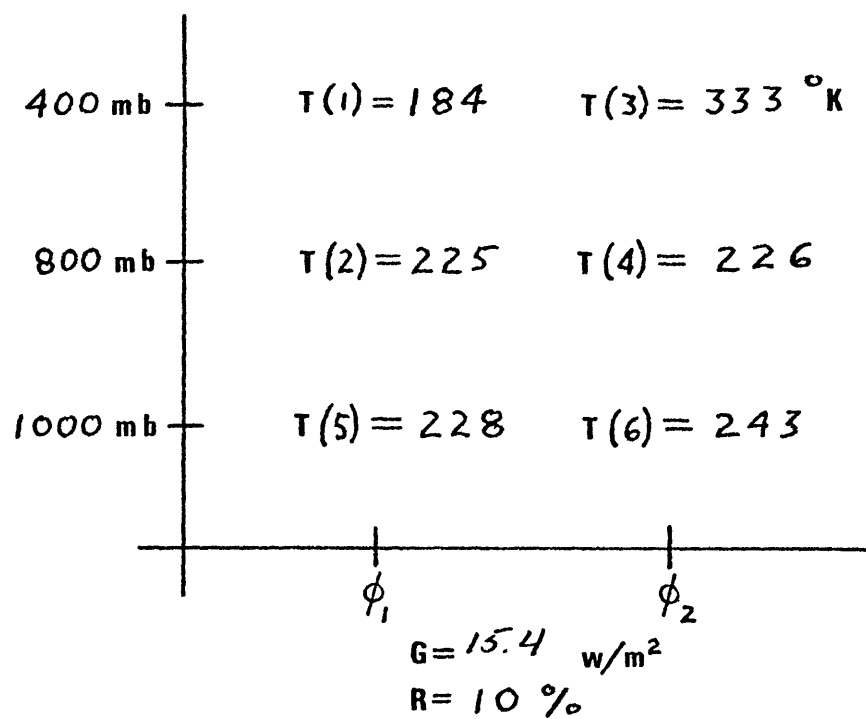


Figure 7

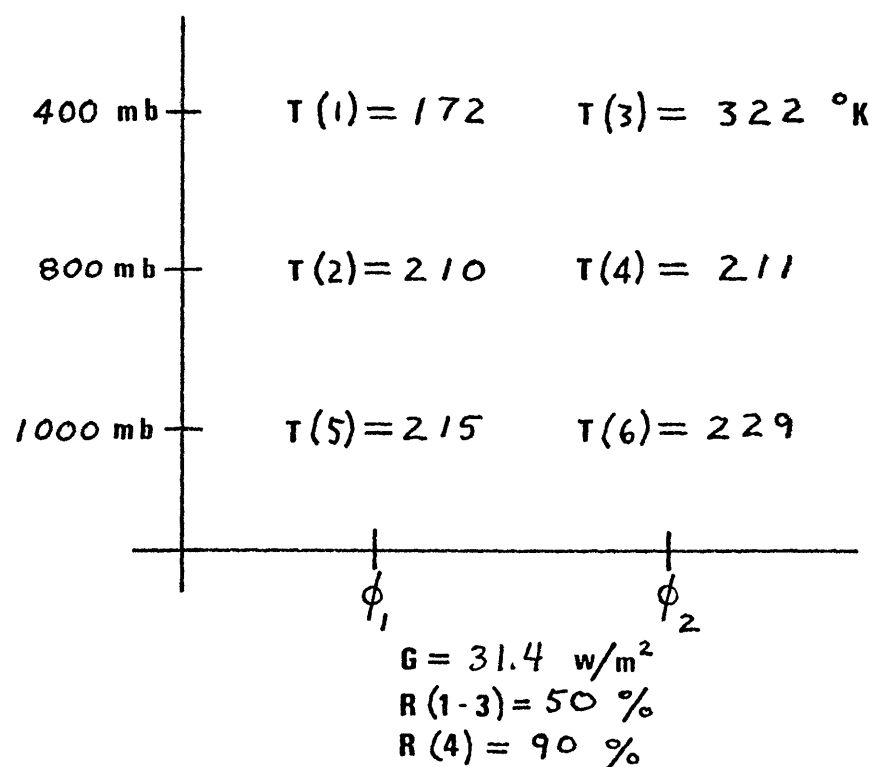


Figure 8



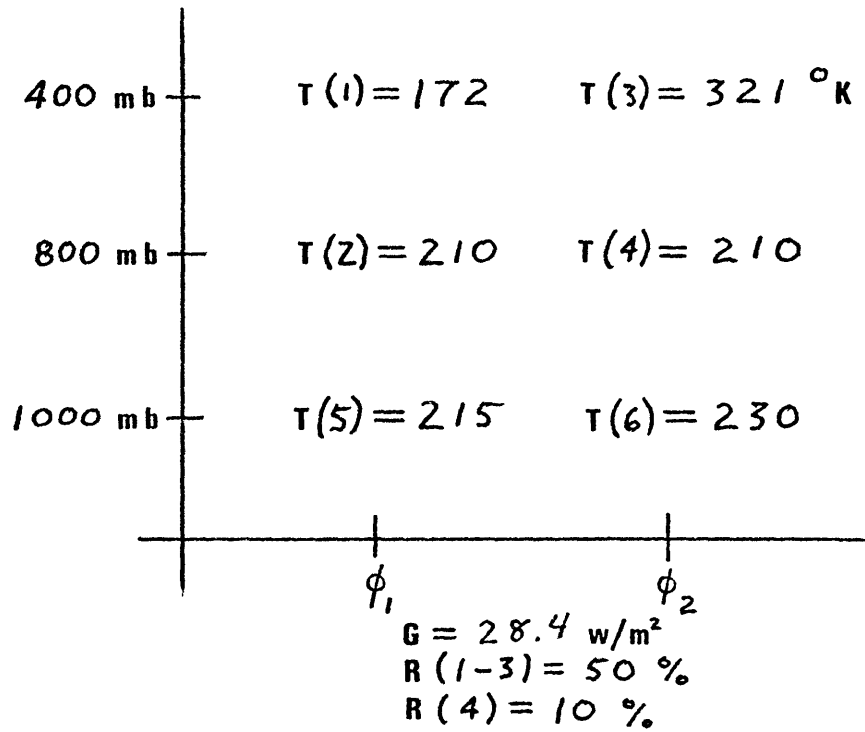


Figure 9

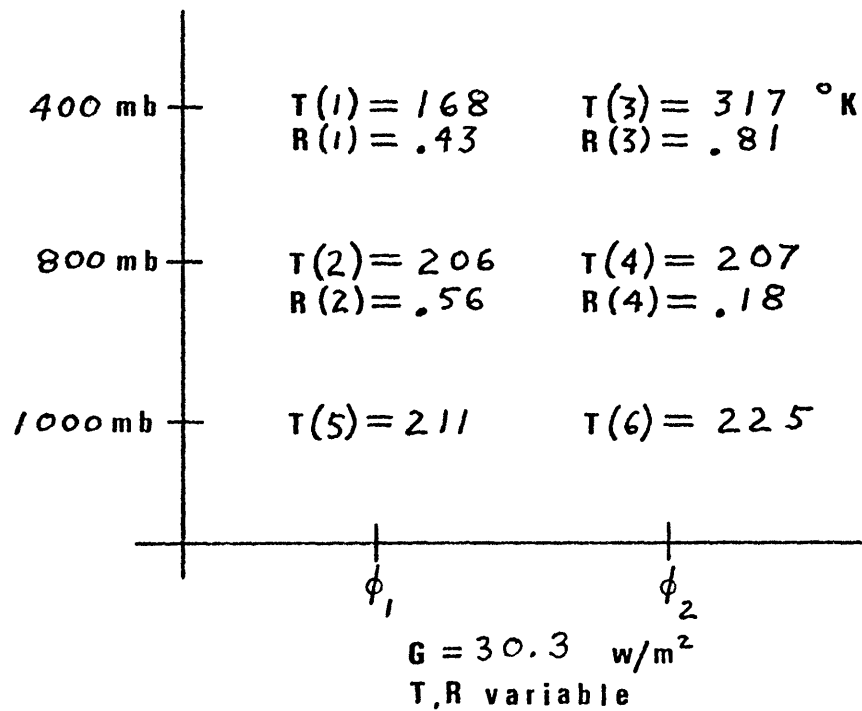


Figure 10

dissimilar to those in figures 5-9. The relative humidities of the poleward latitude are not far from 50% while it appears that a high relative humidity is required for the parcel aloft at the equatorial latitude. The maximum generation was found to be  $G = 30.3 \text{ watts/m}^2$  subject to the constraints on the field of relative humidity. Considering figure 10, we remark the vertically averaged temperature contrast in the meridional direction as being relatively realistic. In the poleward latitude, both temperature and relative humidity decrease with altitude as can be noted in our own atmosphere. The major inconsistency with reality here, is the unusually high value for temperature and relative humidity for parcel number 3. The efficiency that results from this particular distribution of temperature and relative humidity is  $\eta = 8.9\%$ .

## 2. Group #2; Sasamori parameterization of long-wave flux

Figures 11-13 represent the fields which maximize the rate of generation of MAE for a constant relative humidity. This time however, the approximation used for the long-wave fluxes was more realistic than the simple exponential dependence. Figure 11 is for a relative humidity held constant at 50% everywhere. We see immediately that the inversion at 800 mb is no longer present and the field looks fairly realistic. For this case,  $G = 16.6$

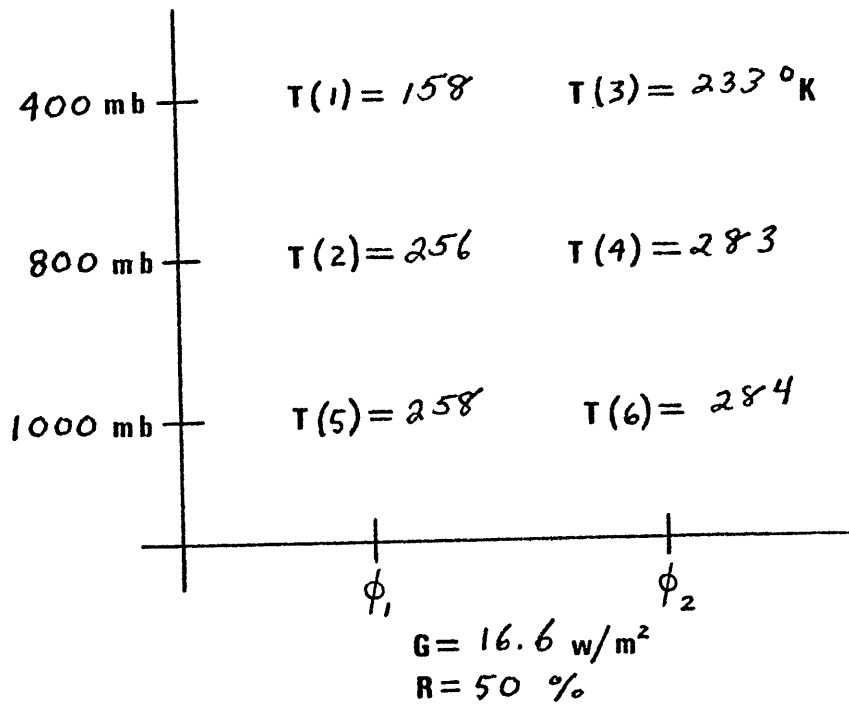


Figure 11

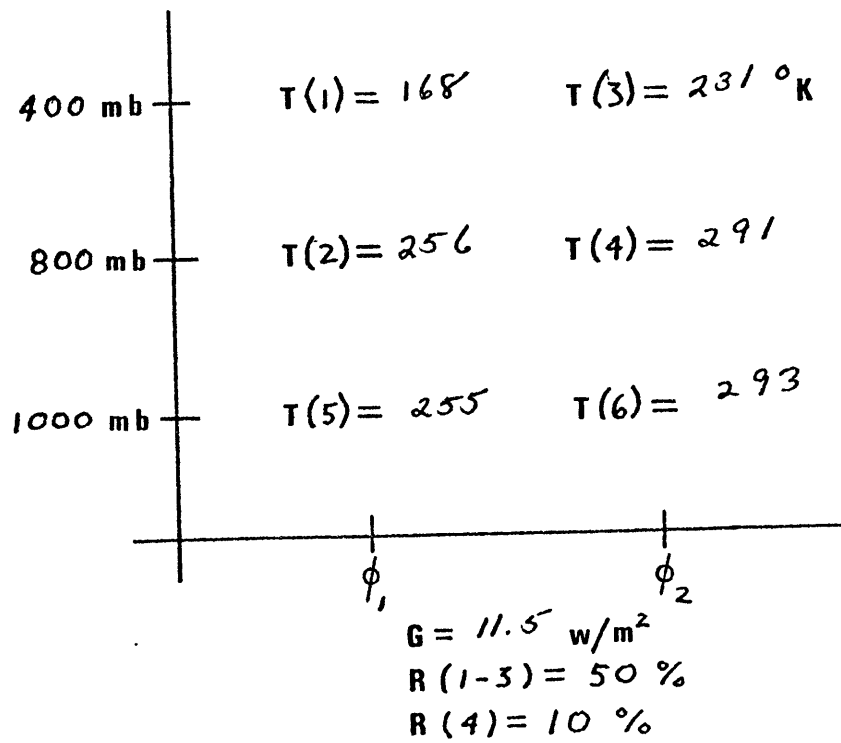


Figure 12

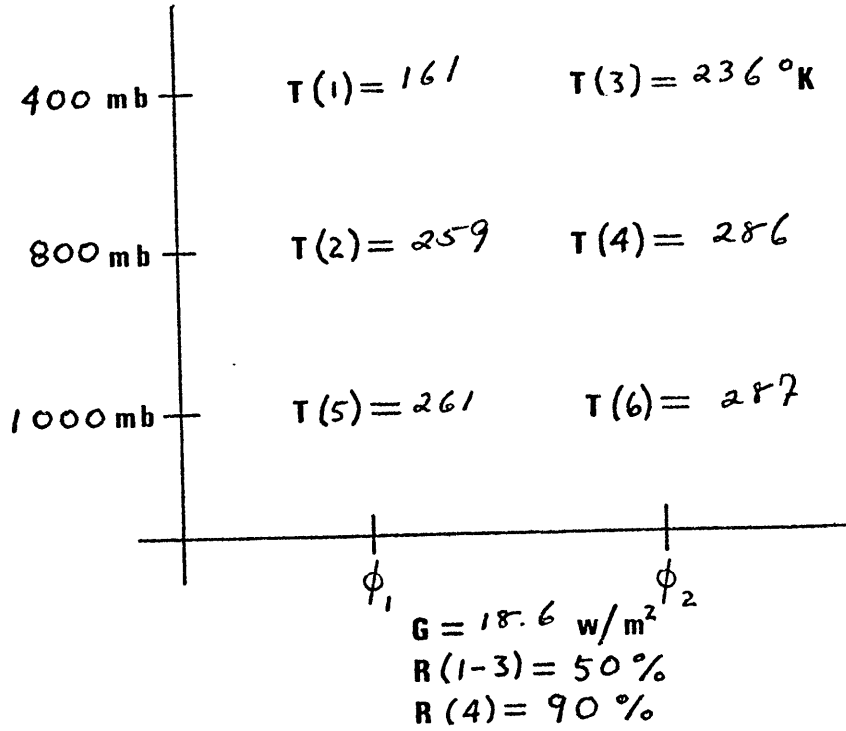


Figure 13

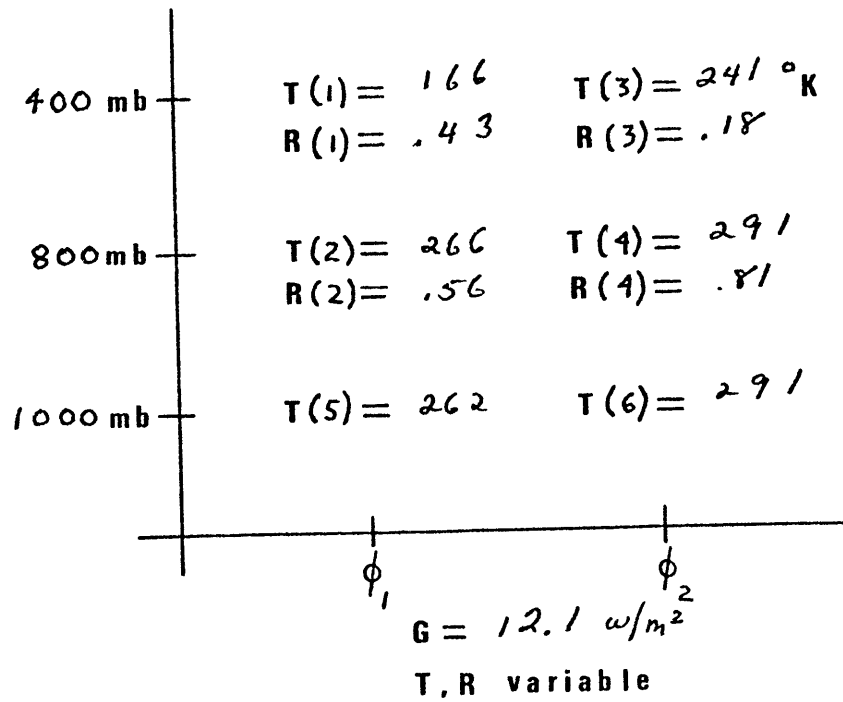


Figure 14

watts/m<sup>2</sup>. In figures 12 and 13, the relative humidity of the fourth parcel is .1 and .9 respectively while the relative humidity is kept at 50% for all other parcels. Unlike the results from group #1, it is clear that the relative humidity of parcel #4 is very influential on the rate of generation of MAE. That is, the high temperature of parcel #4 allows the parcel to hold more water vapor. Because of this, a small change in R(4) will lead to a large change in the water vapor pathlength. For the field in figure 12,  $G = 11.5 \text{ watts/m}^2$  and for figure 13,  $G = 18.6 \text{ watts/m}^2$ . When the field of relative humidity was allowed to vary along with the temperature, the soundings shown in figure 14 represent the necessary distributions to maximize the rate of generation of MAE. The relative humidity field varies subject to the constraint that  $10\% < R(3) < 50\%$ ;  $10\% < R(4) < 90\%$  and  $20\% < R(1,2) < 70\%$ . Now we see that the equatorial latitude shows a realistic gradient of temperature and relative humidity in the vertical. The parcel aloft here is both drier and cooler than the parcel at 800 mb. The horizontal gradient of these two quantities is also similar in sign to the real atmosphere. For the distribution in figure 14,  $G = 12.1 \text{ watts/m}^2$  leading to an efficiency of  $\eta = 3.5\%$ .

In both group #1 and group #2 we note that the maximum rate of generation of MAE for variable temperature and

relative humidity is smaller than  $G$  for  $R(4) = 90\%$  and  $R(1-3) = 50\%$ . This is due to the fact that when  $R$  was allowed to vary, we constrained it to always be less than  $90\%$  but greater than  $10\%$ . The upper bound was chosen because in the real atmosphere, liquid water is present before the relative humidity reaches  $100\%$ . To further reduce the number of possible relative humidity profiles, the relative humidity of parcel #3(4), was constrained to be less than  $50\%$  in group #2(1). Hence, the values of  $G$  in figures 10 and 14, are only the maxima subject to certain constraints upon the field of relative humidity. These constraints were largely necessary because when  $R$  was allowed to vary from  $10\%$ - $90\%$  at the same time that the temperature varied, convergence problems caused the model to fail mid-way. Because of this, it was impossible to get a complete run with both  $T$  and  $R$  ranging to their full extent.

In light of the fact that the maximum rate of generation of MAE was larger for  $R(4) = 90\%$  and  $R(1-3) = 50\%$  than for a variable  $R$  and  $T$ , we recognize that the fields in figures 15 and 18 are for a  $G$  somewhat less than the actual maximum. Presumably, if we had been able to allow the relative humidity of all the parcels to vary from  $10\%$ - $90\%$ , the maximum generation rate would have exceeded  $18.6 \text{ watts/m}^2$ .

## VI. Discussion of Results

In this section the results from the present study will be interpreted and compared to the results obtained by Schulman (1974) and Newell et al (1974). These two studies did not deal with moist available energy directly, but their results for a dry atmosphere may still be used for purposes of comparison.

The results from group #1 are probably not significant enough to be useful in a comparison to past work or observations. The strong and unrealistic inversion present in all of the maximizing fields of this group was thought to be a result of the requirement of the surface flux balance upon the crudely approximated long-wave flux. Hence, we will concern ourselves only with the results in group #2. Before going into the details of comparisons, we will summarize the major assumptions and differences in the past investigations.

In their article on the theory of available potential energy Dutton and Johnson (1967) devised a method of their own for estimating the rate of generation of APE. Their basic equation for the zonally averaged rate of generation

of APE was:

$$\overline{G_z} = \int_{\theta_0}^{\theta_1} \overline{[1 - (P_0/P)^{\kappa}] Q \frac{\partial h}{\partial \theta}} d\theta$$

where  $h$  is a unique inverse function such that

$$h[\theta(x, y, z)] = z$$

This approximate method yielded a  $G = 5.6 \text{ watts/m}^2$ . It is important to note that although the release of latent heat is accounted for, it was treated as a diabatic process.

That is,

$$Q = Q_{\text{rad}} + Q_{\text{latent heating}} + Q_{\text{solar}} + Q_{\text{sensible heating}}$$

Using a more observational approach, Newell et al (1974) suggested a different method for obtaining estimates of the rate of generation of APE. The expression to be solved for  $G$  was:

$$\iiint [\bar{N}] (\overline{[Q_{\text{rad}}]} + \overline{[Q_{\text{LH}}]} + \overline{[Q_{\text{B LH}}]}) d\sigma \frac{dp}{g}$$

Here again, the latent heat release was treated as an external form of heating, along with heating due to long and short-wave radiation and heating from the transport of sensible heat from the surface. The radiational terms were taken from Dopplick (1970) and the latent heat values came from Vincent (1968). In the above equation, the efficiency factor,  $N$ , is not the same one that was used by Lorenz. Here,  $N = 1 - (P_r/P)^{1/2}$

The approximate expression for  $G$  used by Lorenz (1967) was

$$G = \left\{ \Gamma_d (\Gamma_d \tilde{T}) \tilde{T}^{-1} \tilde{Q}'' \tilde{T}'' \right\}$$

where

$$\Gamma = -\partial T / \partial z$$

$$\Gamma_d = g/c_p \sim 10^\circ \text{K / km}$$



( $\sim$ ) = average over an entire isobaric surface

(") = a departure from this average

Using this form for the rate of generation of APE, Lorenz estimated a value of 4 watts/m<sup>2</sup>. The value of the net, zonal rate of generation for the northern hemisphere was  $G = 1.32$  watts/m<sup>2</sup>, while the rate of generation for the entire globe was approximately 3 watts/m<sup>2</sup>.

The third and final study that will be used, is of course the work by Schulman (1974). Although he developed several models which increased in their complexity and resolution, we are only concerned with the results from the 3-level, 2-latitude model with sensible heat included. The atmosphere was treated as thermodynamically dry but aside from that, many of the approximations used are identical to those made in this paper. Latent heat was not parameterized, even as an external heating source since the relative humidity was held fixed at a value less than 100%. As such, the formula used by Schulman was the standard one for the rate of generation of APE with the only difference being that the heating term included only the heating due to radiational effects and sensible heating from the surface. This expression for the rate of generation of APE yielded a rate of 7.8 watts/m<sup>2</sup>. Note that this value is substantially larger than the values estimated by Newell et al and Dutton and Johnson, who both included latent heating in the total diabatic heating. This is not

unexpected since in finding the maximum rate of generation, Schulman effectively found the upper bound, whereas Newell and Dutton and Johnson were finding the actual rate of generation of MAE.

We now consider the fields of temperature and relative humidity which simultaneously maximize the rate of generation of MAE that result from our model. The maximum rate subject to the constrained relative humidity field was found to be  $12.1 \text{ watts/m}^2$ . The temperature and relative humidity fields responsible for this rate are shown in figure 15. For this value of G the efficiency of the atmosphere is 3.5%. In order to ascertain how near to maximum efficiency the real atmosphere is, we must compare the results in figure 15 with the observed distribution of temperature and relative humidity.

Considering the temperature field first, we note that the horizontal meridional temperature gradient is positive towards the equator as is the case in our own atmosphere. The observed temperature gradient at the surface is estimated as  $\sim -1.5 \text{ }^\circ\text{K}/100 \text{ km}$ . This value decreases with increasing altitude in the real atmosphere. In our model the meridional temperature gradient does not decrease appreciably with height and this is thought to be due to lack of resolution.

The sign of the change in temperature in the vertical

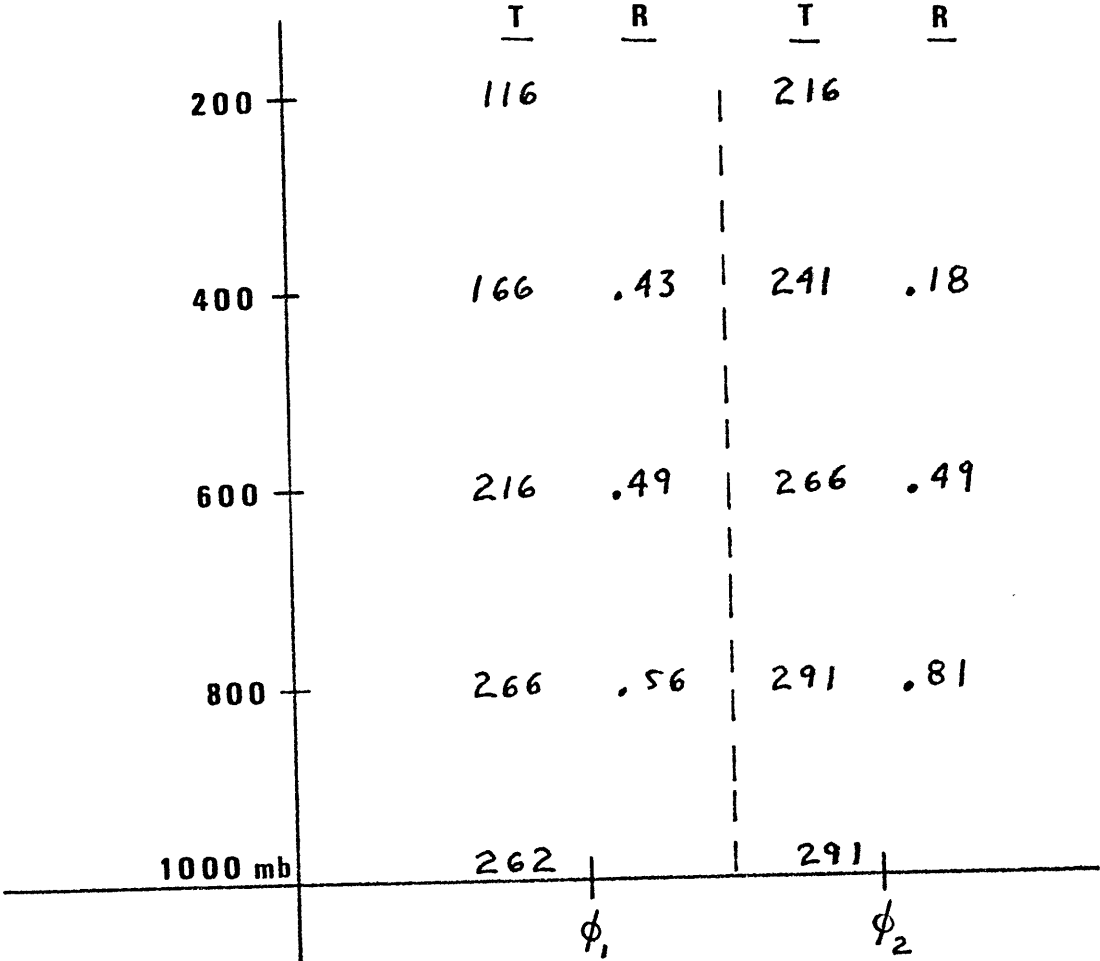


Figure 15

also conforms with the observed gradient. We can see that at both latitudes, the temperature decreases with height. For purposes of comparison figure 16 has been included and represents a cross-section of the real atmospheric temperature distribution by Oort and Rasmussen (1971). Looking at figures 15 and 16, it may be seen that the most important difference is the overall magnitude of the temperature and temperature gradient. The model shows temperature values that at some levels, exceed the observed ones. It is interesting to note that Schulman found that his temperatures were colder than the observed temperature field. The explanation for this was that the low temperature values were due to the large surface temperatures that were required to satisfy the balance constraint at the surface. That is, in order to supply the balancing sensible heat fluxes, large surface temperatures were necessary.

The relative humidity field that was generated by our model appears to display some semblance to the observed distribution. The northern most latitude ( $\phi_1$ ) is fairly dry, showing a slight decrease in relative humidity with increasing height. The southern most latitude ( $\phi_2$ ) on the other hand, has a very large relative humidity near the surface which drops off rapidly with increasing altitude. We must bear in mind, however, that R(3) was constrained

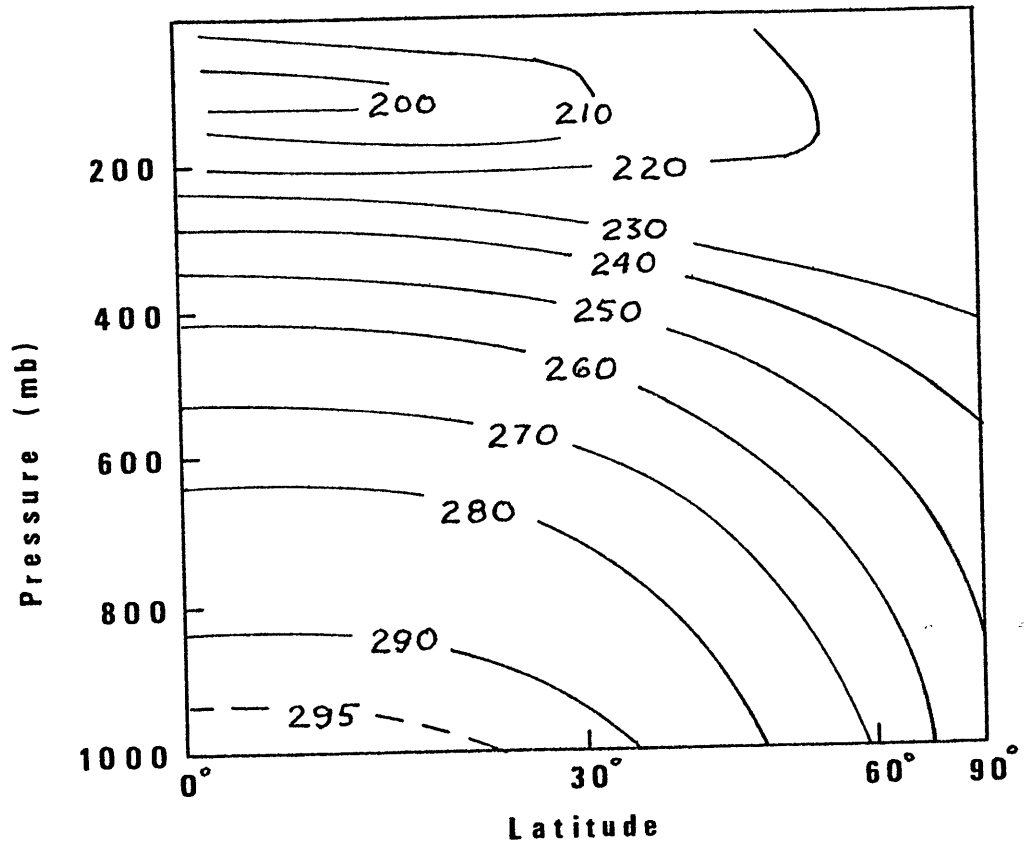


Figure 16

to be less than 50% to start with. Figure 17 displays a cross-section of the observed meridional distribution of relative humidity and again was included for purposes of comparison. We see that the meridional gradient of relative humidity in our model is negative towards the north as in the real atmosphere. The vertical gradient is largest near the tropics in both figures 16 and 17.

The main difference is that the meridional gradient does not decrease with height in our model as it does in the observed case. Furthermore, the magnitudes of the relative humidities aloft do not agree with the observed magnitudes. We may conclude only that the signs of the horizontal and vertical gradients of the relative humidity field in our model bear considerable resemblance to the real atmosphere.

We have seen that the temperature and relative humidity fields which maximize the rate of generation of MAE are in some ways realistic, but now we also want to examine the distribution of heating and the efficiency factor,  $N$ , which result from this distribution. Figures 18 a and b, show the heating and efficiency factor distributions that lead to the maximum  $G$ . Consider first the heating,  $Q$ .

We can see from figure 18a that  $Q$  is positive at both levels at the equatorward latitude. At the poleward latitude, there appears to be cooling at both levels. The

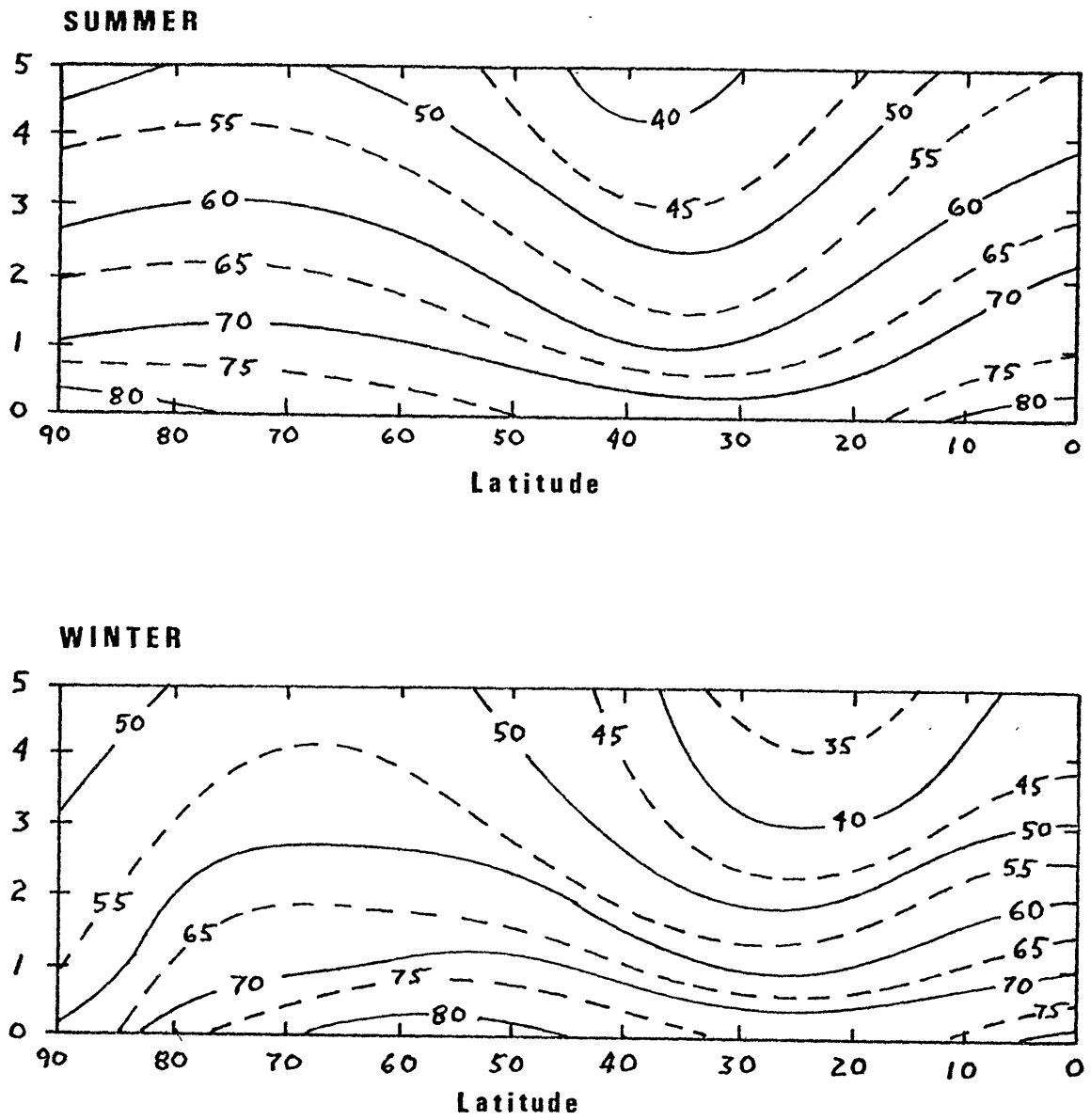


Figure 17

maximizing Q - field obtained by Schulman (1974) for a dry atmosphere, was quite different. Schulman's field showed heating at 800 mb at both latitudes and cooling aloft. The overall magnitude of his values were larger than those generated by the present model. Possibly, this is due to the fact that Schulman did not allow for the presence of any saturated air. This of course would allow for greater heating.

Looking at figure 18b, we consider the maximizing distribution of the efficiency factor, N. Apparently,  $N < 0$  only for parcel #1, the parcel aloft at  $\phi_1$ . Again, this differs from the results that Schulman obtained. His field indicated that  $N > 0$  for both parcels at the equatorward latitude while  $N < 0$  for  $\phi_1$ . Hence, Schulman concluded that most of the APE was generated near the surface at the equatorward latitude. Our results, however, imply that MAE is being generated near the surface at  $\phi_2$  and aloft at  $\phi_1$  and  $\phi_2$ . We may compare this result with figure 19 after Lorenz (1978). From this figure it is clear that Lorenz also found that MAE is mainly generated near the surface in the tropics and is largely destroyed near the surface at the pole. The main difference then, between our results and Lorenz's, is the large generation of MAE aloft at  $\phi_2$ .

In figures 20 and 21, we can see the observed Q and N



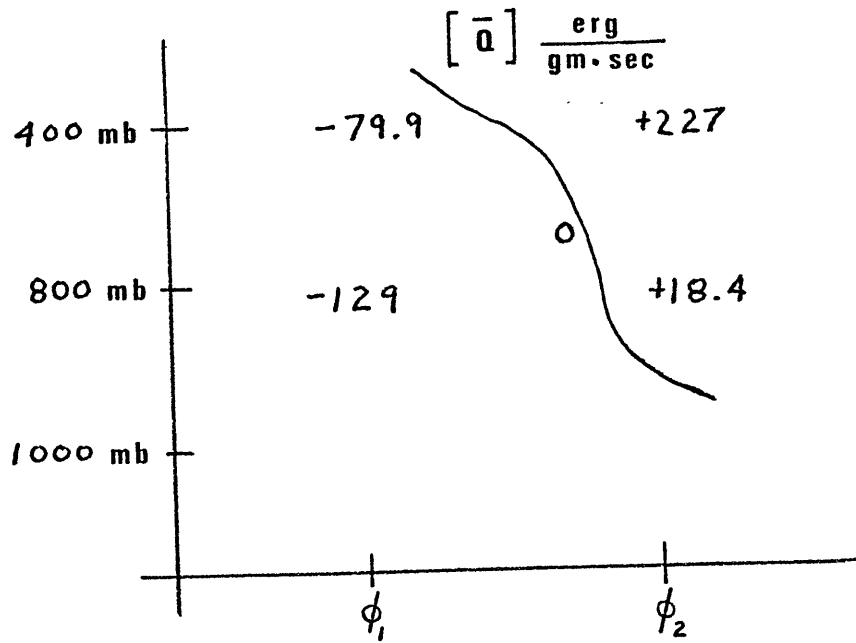


Figure 18 a

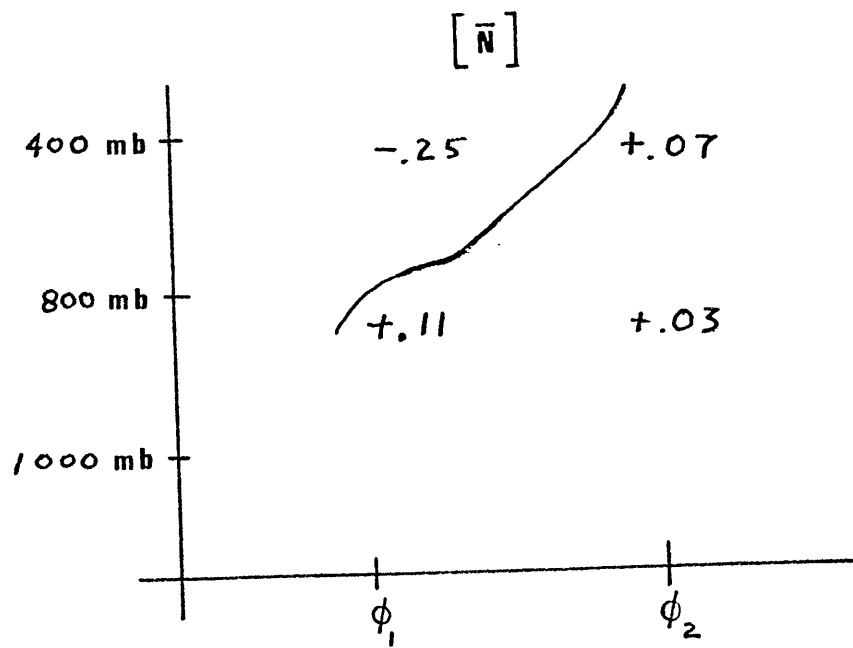


Figure 18 b

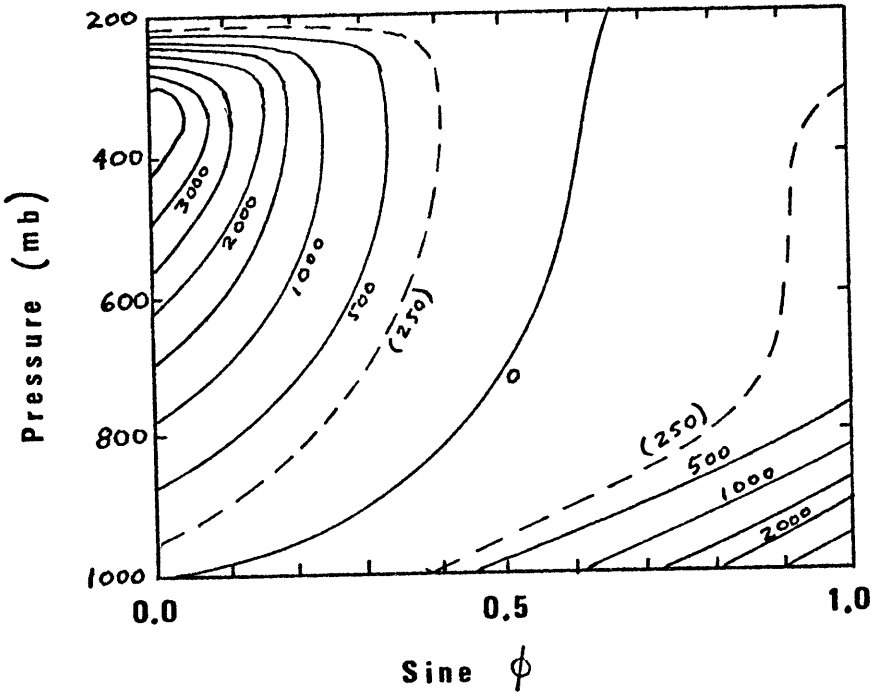


Figure 19

fields after Newell et al (1974). The  $Q$  term here however, is the net heating for summer and winter, including the latent heating. Hence, we can compare figure 18a with figure 20 only to a limited extent.

Comparing figure 18a with figure 20, it is difficult to draw conclusions because in figure 18a, the heating is presumed to be entirely due to long-wave fluxes and sensible heating at the surface. Figure 20 shows cooling near the surface at  $\phi_2$  and aloft at  $\phi_1$ . Heating occurs at the surface at  $\phi_1$  and aloft at  $\phi_2$ . The most obvious disagreement is the unrealistically large amount of heating at parcel #3 in our model. This is really quite different from figure 18a. Considering the simplicity of our model, this is perhaps not unexpected. Similarly, figures 18b and 21 are not in exact agreement either although they both indicate a positive efficiency at 800 mb at  $\phi_2$  and a negative efficiency at 400 mb at  $\phi_1$ .

We must bear in mind, that both Schulman and Newell have treated an essentially dry atmosphere so that we would expect differences between their results and our own. Furthermore, in Schulman's model, no parcels ever got saturated since all parcels were constrained to remain on the dry adiabat at all times. Hence, the rate of heating and cooling in Schulman's model was quite different from the ones in the present model.

The major differences between our maximizing fields and

$Q_{net}$  ( $^{\circ}\text{C}/\text{day}$ )

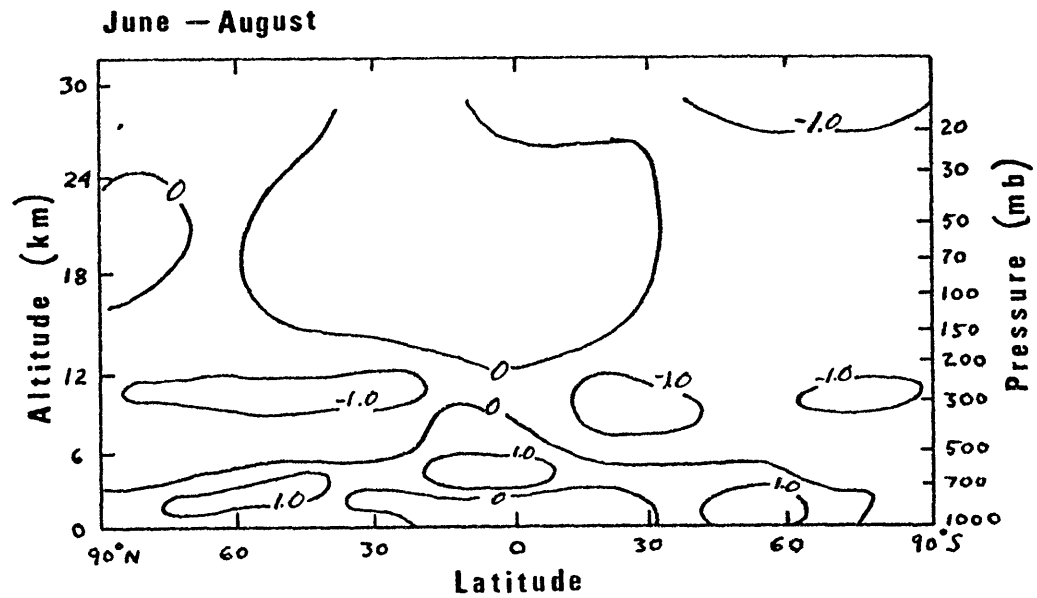
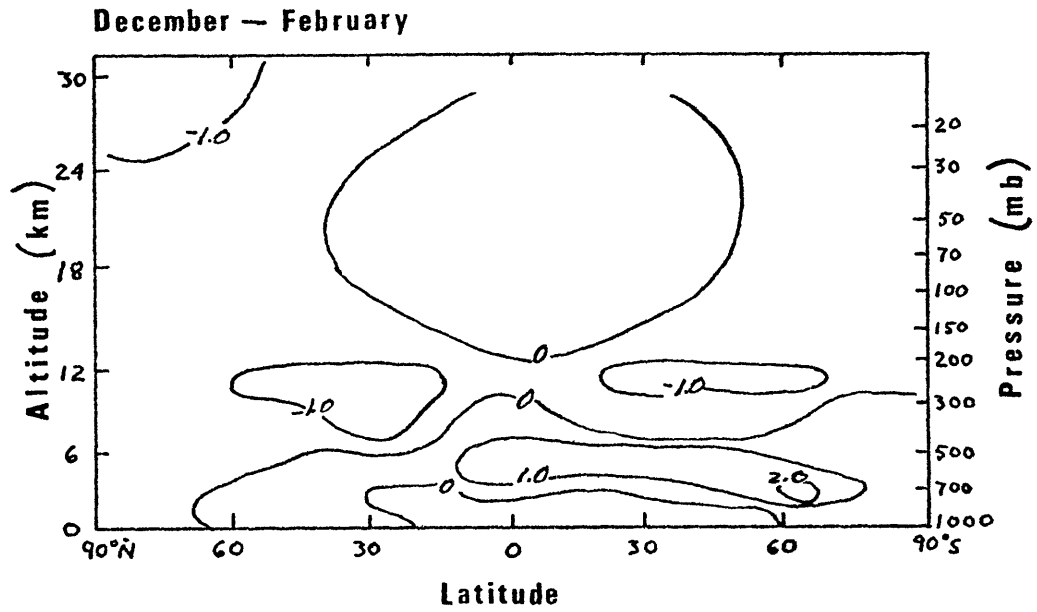


Figure 20

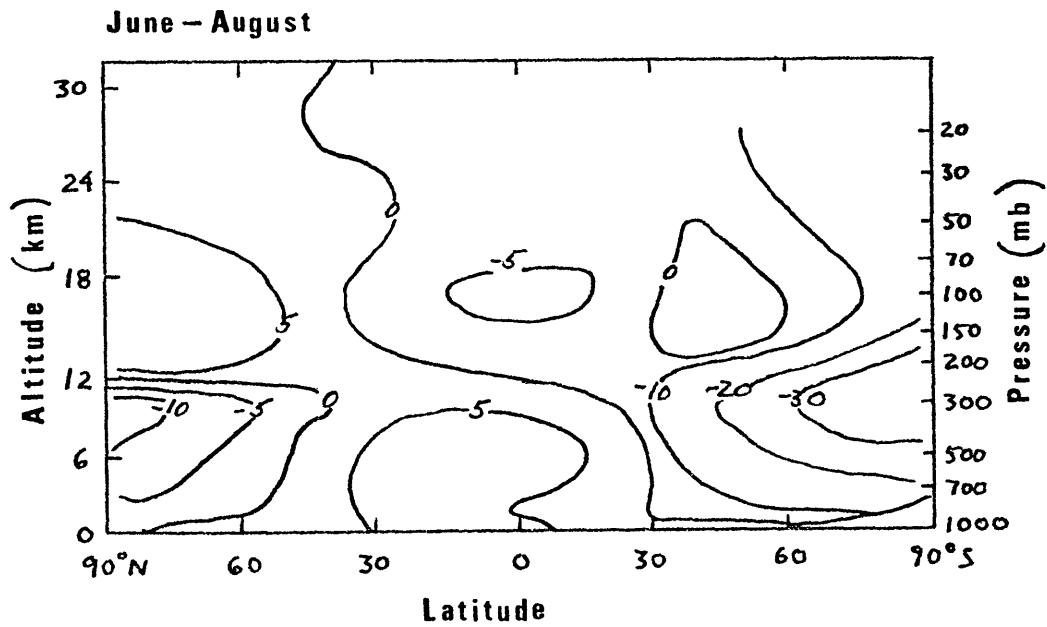
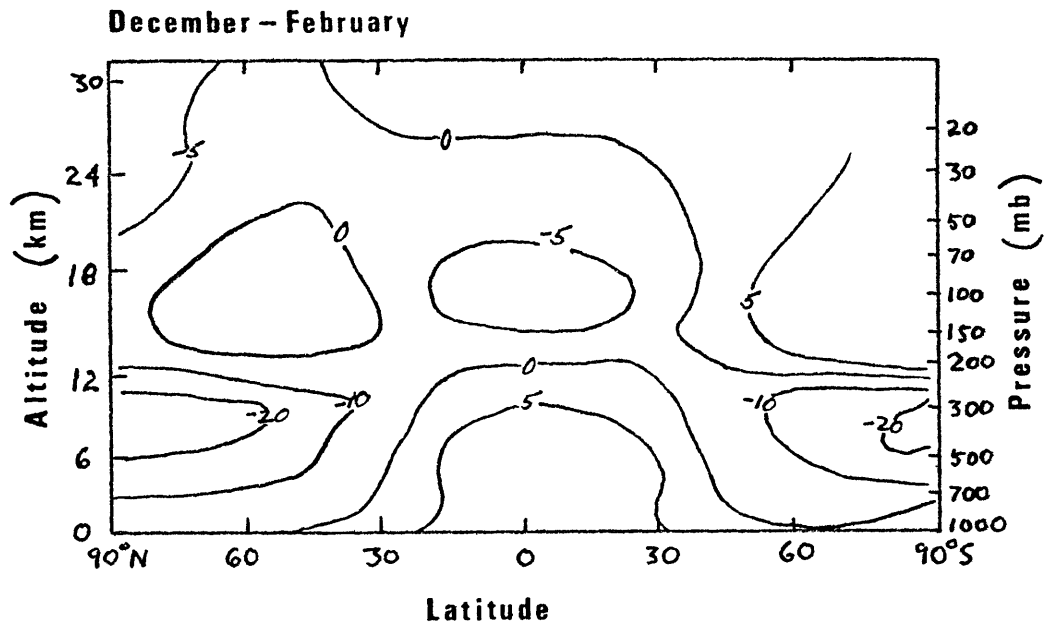


Figure 21

those in the real atmosphere lie mainly in the distribution of heating and also in the temperature and efficiency fields. The unrealistic features in those fields generated by the model are thought to be largely due to the parameterization of the long-wave fluxes. The Sasamori equations used are really only valid for temperatures between about 200 - about 340 °K. Some of the temperatures generated by the model are as low as 158°K. Furthermore, the Sasamori approximation may not be appropriate for a simple 4-point atmosphere. That is, the equations are generally used in models where the atmosphere has several layers in the vertical - not two individual points. The Sasamori equations can be used to estimate the long-wave radiation from a layer of finite thickness, not the radiation from a point. Reflecting on the differences between the hypothetical atmosphere in the model and the observed atmosphere, there is some question as to the justification of using such a complex parameterization in such a simplified model.

The rather high efficiency that the present model yielded was thought to be mainly due to the particular assumptions made in the model. For example, sensible heat was included near the ground, but the transfer of sensible heat by the turbulent eddies into the upper atmosphere was not parameterized. The moist processes were included when parcels ascended and descended but evaporation and precip-

itation were not parameterized. Similarly, we did not include latent heat release as a form of external heating, but we avoided it by constraining the relative humidities to be less than 90%. Hence, the contribution of latent heat energy to the generation of MAE was not accounted for. It is possible that if evaporation and precipitation were treated, that the atmospheric efficiency would have been altered. This would be especially true in light of Lorenz's (1978) findings that evaporation (precipitation) is very efficient at creating (destroying) moist available energy.

## VII. Summary and conclusions

By examining the maximum possible rate of generation of moist available energy, this thesis has investigated the efficiency of a moist atmosphere. In this way, we need not handle the problem of determining the atmospheric motions from which the maximum rate of generation of MAE results. Lorenz (1955b) and Schulman (1974) used this basic approach to examine the efficiency of a dry atmosphere and found that the atmosphere may well be operating near maximum efficiency. This paper has been an attempt at combining the more recent work on MAE by Lorenz (1978) with past investigations of the atmospheric efficiency.

Several assumptions were made to simplify the problem. Besides ignoring ozone in the atmosphere and assuming that all atmospheric heating was accomplished by long-wave radiation only, it was assumed that the relative humidity was always less than 90% so that the processes of precipitation and evaporation were eliminated. Hence, we were able to treat the atmospheric efficiency as a function of temperature and relative humidity alone. Our task was then reduced to finding those distributions of temperature and relative humidity which simultaneously maximized the rate of generation of MAE.

The model that was developed to determine the rate of generation of MAE, was a 2-dimensional one, since it was



assumed that the solar forcing is essentially a function of latitude and not longitude. A series of runs was made using this model, first with a constant relative humidity and then with both the temperature and relative humidity as variables. The maximum efficiencies ranged from less than 1% to near 3%.

In the first series of runs where the relative humidity was held constant, the characteristics of the temperature field leading to the maximum rate of generation, bore some resemblance to the observed temperature distribution. Specifically, the sign of the horizontal and vertical temperature gradients were relatively realistic. Furthermore, when the relative humidity of parcel #4 was varied by itself, it was clear that  $G$  was very sensitive to this value.

When both the temperature and relative humidity were allowed to vary, the resulting temperature and relative humidity distributions bore stronger resemblances to the features of the observed atmosphere. The equatorward latitude showed the largest value of moisture near the surface and the steepest gradient of relative humidity in the vertical.

Considering the fact that observational studies indicate an atmospheric efficiency of 1-2%, it is difficult to say whether or not the results of this thesis support

the hypothesis that the atmosphere is operating near a maximum efficiency. Certainly we would not be justified in claiming that, based on these findings, the atmosphere is not running near maximum efficiency. In light of the fact that the maximizing fields of temperature and relative humidity do not differ too drastically from the observed fields, we may conclude that our results lean towards supporting the initial hypothesis rather than disproving it. It is felt that the unusually high efficiencies generated by the model are not unexpected due to the lack of resolution and crudeness of some of the assumptions made. When we consider in addition, the possibly unjustified use of the Sasamori equations for the long-wave radiation, highly realistic values for the maximizing fields cannot be expected. The results do indicate that there is a need for an alternate parameterization of the long-wave flux which is less complex than the Sasamori approximation but more realistic than the simple exponential approximation first used in the model. The development of such a parameterization was not pursued in this paper and goes beyond the scope of the investigation presented here.

The next step in pursuing an investigation of the atmospheric efficiency, would be to parameterize the latent heat energy and hence the processes of evaporation and condensation. This is not only a modelling problem, but

one of deciding where and when such processes will take place. In addition, with no constraints on the relative humidity, the presence of clouds must be accounted for. However, now that the concept of MAE has been developed, it is perhaps not as great a task to investigate the efficiency of an atmosphere including clouds and latent heat energy, as it might have been in the past.

APPENDIX

In the cases where the Sasamori equations were used to approximate the long-wave flux, the trapezoidal method was implemented to solve the integrals. Below is an example showing the calculation of the upward and downward flux across a parcel at 400 mb:

$$F_{IU}(\phi) = \sigma(\bar{T}_g(\phi))^4 - 2\sigma \left[ \bar{A}_0 (u(\bar{T}_{800}) - u(\bar{T}_{400})) \bar{T}_{800}^3 (\bar{T}_g(\phi) - \bar{T}_{600}) \right]$$

$$F_{ID}(\phi) = 2\sigma \left[ \bar{A}_0 (u(\bar{T}_{400}) - u(\bar{T}_{200})) \bar{T}_{200}^3 (\bar{T}_{400} - \bar{T}_{200}) \right]$$

while the net long-wave flux out of the top of a column at a given latitude would be:

$$F_{net \uparrow}(\phi) = \sigma(\bar{T}_g(\phi))^4 - 2\sigma \left[ \bar{A}_0 [u(\bar{T}_{800}) - u(\bar{T}_{200})] \bar{T}_{800}^3 (\bar{T}_g(\phi) - \bar{T}_{600}) \right. \\ \left. + \bar{A}_0 [u(\bar{T}_{400}) - u(\bar{T}_{200})] \bar{T}_{400}^3 (\bar{T}_{600} - \bar{T}_{200}) \right]$$

### Acknowledgements

I should like to extend thanks to Professor Edward N. Lorenz whose advice and suggestions greatly aided the completion of this study.

I am grateful to Dr. Ron Errico for being so generous with his time in discussing some of the hang ups that presented themselves in this topic.

Additionally, sincere thanks are extended to George A. Silvis who did the drafting for this thesis, and to Patty Farrell for typing the manuscript.

My financial support in the department was in part provided by grants from the National Science Foundation and the U.S. Airforce, contract numbers NSF-G 77 10093 ATM and AF F19628-78-C-0032.

References

- Brunt, D., 1926: Energy in the Earth's Atmosphere. Phil. Mag., 7, 523-532.
- Colman, Bradley, R., 1978: Special Prob's paper.
- Dutton, J. A. & D. R. Johnson, 1967: The theory of available potential energy and a variational approach to atmospheric energetics. Advances in Geophysics, 12, Academic Press, New York, 333-436.
- Holopainen, E. O., 1963: On the dissipation of kinetic energy in the atmosphere. Tellus, 15, 26-32.
- Kraus, E. B., 1972: Atmosphere-Ocean Interaction. Clarendon Press, Oxford, 275 pp.
- Kung, E. C., 1966: Large-scale balance of kinetic energy in the atmosphere. Mon. Weather Rev., 94, 627-640.
- Kung, E. C., 1969: Further study on the kinetic energy balance. Mon. Weather Rev., 97, 573-581.
- Lettau, H., 1954: A study of the mass, momentum, and energy budget of the atmosphere. Archiv. Meteor. Geophys. Bioclima., A, 7, 133-157.
- Lorenz, E. N., 1955a: Available potential energy and the maintenance of the general circulation. Tellus, 7, 157-167.
- Lorenz, E. N., 1955b: Generation of available potential energy and the intensity of the general circulation. Univ. Calif. at Los Angeles, Dept. of Meteor., #AF 19(604) - 1286, 35 pp.

- Lorenz, E. N., 1967: The Nature & Theory of the General Circulation of the Atmosphere. Tech. Note No. 218, TP115, WMO, Geneva, 161 pp.
- Lorenz, E. N., 1978: Available energy and the maintenance of a moist circulation. *Tellus*, 30, 15-31.
- Manabe, S. and R. T. Wetherald, 1967: Thermal Equilibrium of the Atmosphere with a given Distribution of Relative Humidity. *Journal of Atmos. Sciences*, 24, 3, 241-259.
- Margules, M., 1903: *Über die Energie der Stürme*. *Jahrb. Zentralansh. Meteor.*, Vienna, 1-26.
- Newell, R. E., J. W. Kidson, D. G. Vincent and G. J. Boer, 1972: The General Circulation of the Tropical Atmosphere and Interactions with Extra tropical Latitudes. M.I.T. Press, Cambridge.
- Oort, A. H. and E. M. Rasmusson, 1971: *Atmospheric Circulation Statistics*. NOAA Professional Paper 5, U.S. Dept. of Commerce, Nat. Oceanic and Atmos. Adm., Rockville, Maryland, 323 pp.
- Sasamori, T., 1968: *The Radiative Cooling Calculation for Application to General Circulation Experiments*. *J. Appl. Met.*, 7, 721-729.
- Schulman, Lloyd, L., 1974: *A Theoretical Study of the Efficiency of the General Circulation*. Ph.D. Thesis M.I.T.
- Wojcik, Michael, A., 1977: *Sensitivity of Moist Available Energy to Increase in Temperature*. S.M. Thesis, M.I.T.

Wulf, O. R. and L. Davis, 1952: On the Efficiency of the engine driving the atmospheric circulation.

J. Met., 9, 79-82.

Yamamoto, G., 1952: On a radiation chart. Sci. Rept.,

Tohoku Univ., Ser. 5, Geophys., 4, 9-23.